Modeling of Inertial Multi-Phase Flows through High Permeability Porous Media: Friction Closure Laws

Rémi Clavier, Nourdine Chikhi, Florian Fichot, Michel Quintard

Modeling of inertial multi-phase flows through high permeability porous media: Friction closure laws

R. Clavier [a,*], N. Chikhi [a], F. Fichot [b], M. Quintard [c]

[a] *Institut de Radioprotection et de Sûreté Nucléaire (IRSN) - PSN-RES/SEREX/LE2M - Cadarache bât. 327 - 13115 St Paul-lez-Durance, France*
[b] *Institut de Radioprotection et de Sûreté Nucléaire (IRSN) - PSN-RES/SAG/LESAM - Cadarache bât. 700 - 13115 St Paul-lez-Durance, France*
[c] *Institut de Mécanique des Fluides de Toulouse (IMFT) - Université de Toulouse, CNRS-INPT-UPS, Toulouse France*

Keywords:
Multi-phase flow
Inertial
Nuclear safety
Debris bed
Reflooding
Porous media

A B S T R A C T

During a severe accident in a nuclear reactor, the core may be fragmented in a debris bed made of millimetric particles. The main safety procedure consists in injecting water into the core leading to a steam-water flow through a hot porous medium. To assess the coolability of debris bed, there is a need for an accurate two-phase flow model including closure laws for the pressure drop. In this article, a new model for calculating pressure losses in two-phase, incompressible, Newtonian fluid flows through homogeneous porous media is proposed. It has been obtained following recent developments in theoretical averaging of momentum equations in porous media. The pressure drops in the momentum equations are determined by eight terms corresponding to the viscous and inertial friction in liquid and gas phases, and interfacial friction between the phases. Analytical correlations with the void fraction have been formulated for each term using an original experimental database containing measurements of pressure drops, average velocities and void fractions from the IRSN CALIDE experiment. The new model has then been validated against the experimental data for various liquid and gas Reynolds numbers up to several hundreds. Finally, it has been compared to the models, usually used in the "severe accident" codes, which are based on a generalization of the Ergun law for multi-phase flows. The results show that the new model gives a better prediction both for the pressure drop and for the void fraction.

1. Context

The modeling of multi-phase flows in porous media is of great interest in many scientific and industrial fields, such as chemical engineering, petroleum engineering, environmental sciences or geology. The pore-scale physics is very complicated, on one hand because of the multiple variables affecting the flow (Capillary, Bond and Reynolds numbers, wettability, viscosity ratio, ...), on the other hand because of the complex pore-scale geometry. Most of the literature is concerned by creeping flows in media of moderate or low permeability for which capillarity is the dominant process. Two-phase flows in high permeability media (typically a pore-scale characteristic length of several millimeters or larger), however, are encountered in many applications, for instance, in chemical engineering (packed bed with large grain size, structured packings, ...), nuclear safety. This latter application has triggered several studies in the wake of the Three Mile Island-2 reactor accident in 1979 (Broughton et al., 1989). In Light Water Reactor (LWR) nuclear safety analysis, specific models are required for describing boiling water-steam flows through particle beds in order to assess the coolability of nuclear fuel debris beds that may be formed during a severe accident in a nuclear reactor, after mechanical failure of the fuel assemblies. For example, the formation of a several-tons debris bed has been reported after the Three Mile Island-2 reactor accident, the bed being characterized by millimetric particle sizes and a porosity ranging from 0.35 to 0.55.

A nuclear fuel debris bed, referred to below as *debris bed*, can be described as a hot porous medium, where substantial amounts of energy are released due to the radioactive decay of fission products. The generated heat has to be extracted from the debris bed in order to stop the progression of the accident. The main safety procedure consists in injecting water into the bed. Given the high permeability of the porous bed and the strong thermal effects, the resulting flow of steam and water through such a hot porous medium can not be predicted on the basis of current knowledge and understanding. Therefore, accurate models are required to reduce the uncertainties concerning the assessment of the debris coolability.

* Corresponding author.
E-mail addresses: remi.clavier@irsn.fr, remi.clavier@cea.fr (R. Clavier), nourdine.chikhi@irsn.fr (N. Chikhi).

Nomenclature

Latin

d	Diameter of the particles used in experiments (m)
F_i	Interfacial friction term in generalized Ergun models (Pa/m)
$\mathbf{F}_{\beta\beta}$	Inertial correction tensor for the β-phase
$F_{\beta\beta}$	Component of $\mathbf{F}_{\beta\beta}$ for 1D flows
$f_{\beta\beta}$	Empirical function in the model proposed for $F_{\beta\beta}$
$\mathbf{F}_{\beta\gamma}$	Inertial coupling tensor of the γ phase over the β-phase ($\beta \neq \gamma$)
$F_{\beta\gamma}$	Component of $\mathbf{F}_{\beta\gamma}$ for 1D flows
$f_{\beta\gamma}$	Empirical function in the model proposed for $F_{\beta\gamma}$
g	Acceleration due to gravity (m/s^2)
K	Permeability (m^2)
K_β	Relative permeability for the β-phase (-)
$\mathbf{K}_{\beta\beta}$	Permeability tensor for the β-phase
$K_{\beta\beta}$	Component of $\mathbf{K}_{\beta\beta}$ for 1D flows
$k_{\beta\beta}$	Empirical function in the proposed model for $K_{\beta\beta}$
$\mathbf{K}_{\beta\gamma}$	Viscous coupling tensor of the γ phase over the β-phase ($\beta \neq \gamma$)
$K_{\beta\gamma}$	Component of $\mathbf{K}_{\beta\gamma}$ for 1D flows
$k_{\beta\gamma}$	Empirical function in the proposed model for $K_{\beta\gamma}$
n	Exponent appearing in the expression of f_{lg} (empirical)
$\langle p_\beta\rangle^\beta$, P_β	Intrinsic average pressure within the β-phase (Pa)
dP/dz	Average pressure gradient in experiments (Pa/m)
Re_β	Reynolds number of the β-phase (-)
$\langle v_\beta\rangle$	Average velocity of the β-phase (filtration velocity) in a 1D flow (m/s)
$\langle \mathbf{v}_\beta\rangle$	Average velocity vector of the β-phase

Greek

α	Void fraction, or gas saturation, in a gas-liquid flow (-)
ε	Porosity (-)
η	Passability (m)
η_β	Relative passability for the β-phase (-)
μ_β	Dynamic viscosity of the β-phase (Pa.s)
ρ_β	Density of the β-phase (kg/m^3)

Integral 0D/1D models for steam-water boiling flows in porous media, involving averaged conservation equations - mass, energy, momentum- and closure laws -for the energy and momentum equations-, have been developed and extended afterwards to 2D/3D situations, assuming homogeneity and isotropy conditions for the debris bed (Fichot et al., 2006). Their validation is based on predictions of global parameters (steam production, bed temperature) measured in integral experiments of debris bed cooling: dry-out heat flux, in dry-out experiments (Decossin, 1999; Dhir and Catton, 1977; Hardee and Nilson, 1977; Lipinski, 1984), or quench front progression velocity, in reflood experiments -top flooding (Cho et al., 1984; Ginsberg et al., 1982; Tung and Dhir, 1988; Tutu et al., 1984b) or bottom flooding (Hall and Hall, 1981; Tung and Dhir, 1986; Tutu et al., 1984a), and global steam production. The available models are based on the use of macro-scale equations for energy or momentum balances based on separate closures, e.g. the macro-scale momentum equations are those developed for isothermal conditions at the closure level, i.e., the macro-scale structure and the related effective properties are those of isothermal flows, while the macro-scale equations are used of course under non-isothermal conditions. While this separation in the upscaling from the pore-scale to macro-scale may be questionable and has not been fully validated, it seems to produce acceptable predictions (Fichot et al., 2006). At this time, given the range of parameters involved in flow through highly permeable media, especially in the context of nuclear safety, a validation of the uncoupled closures has not even been obtained yet, because of the lack of experiments where thermal and mechanical effects are separated.

Indeed, the experimental data cited above have been performed mainly under atmospheric pressure in thermal-hydraulic conditions representative of a severe accident in a nuclear reactor. They correspond to water filtration velocities ranging from 5 mm/s to 32 mm/s and gas filtration velocities ranging from 1 m/s to 7 m/s (Clavier, 2015). In this context, a new experimental dataset has been recently reported by Chikhi et al. (2016), which contains measurements of pressure drop and void fraction versus velocities for high velocity air-water flows through particle beds representative of debris beds. These data emphasized some lack of predictability of the current closure laws used in severe accident simulation codes, and pointed out the need of new models to describe high velocity two-phase flows through debris beds. The objective of this article is to present a new modeling approach for such flows. The mathematical form of the model is obtained from recent results based on volume averaging of the local conservation equations and will be presented in Section 2. Using experimental data presented in Section 3, new correlations for the effective parameters in the model will be derived in Section 4 and validated in Section 5.

2. Theoretical background

2.1. Macroscopic momentum equations for two-phase flows in porous media

In nuclear safety studies, considering the thermal-hydraulic conditions and range of permeability of the debris beds, relatively high, substantial inertial effects and small capillary effects are expected. Thus, the models generally used in severe accident codes are based on heuristic generalizations of Darcy–Forchheimer equations to two-phase flows (Fichot et al., 2006; Lipinski, 1981; Reed et al., 1986; Schulenberg and Müller, 1987; Tung and Dhir, 1988). A possible although not unique formulation of these models is:

$$-\frac{\partial \langle p_l\rangle^l}{\partial z} - \rho_l g = \frac{\mu_l}{KK_l}\langle v_l\rangle + \frac{\rho_l}{\eta\eta_l}\langle v_l\rangle^2 - \frac{F_i}{\varepsilon(1-\alpha)} \quad (1)$$

$$-\frac{\partial \langle p_g\rangle^g}{\partial z} - \rho_g g = \frac{\mu_g}{KK_g}\langle v_g\rangle + \frac{\rho_g}{\eta\eta_g}\langle v_g\rangle^2 + \frac{F_i}{\varepsilon\alpha} \quad (2)$$

where $\langle p_\beta\rangle^\beta$ denotes the intrinsic average pressure, $\langle v_\beta\rangle$ is the average velocity, or *filtration velocity*, ρ_β and μ_β are the density and the viscosity of the fluids, the index β denoting the phase l for the liquid and g for the gas. Parameters ε and α respectively denote the porosity of the medium and the void fraction. Porosity is the ratio between the volume of the pore space and the total volume occupied by the porous medium. In a gas-liquid flow, void fraction designates the volume fraction of the pore space which is occupied by the gas.[1] The norm of the gravity acceleration (upward z-axis) is noted g. Parameters K and η denote the *permeability* and *passability* of the debris bed, as defined in Ergun's law (Ergun, 1952). K_l and K_g are the *relative permeabilities*, η_l and η_g are the *relative passabilities*, and they all depend at least on the fluid saturation. The term F_i was introduced heuristically to account for the effect

[1] The notion of void fraction is largely employed in nuclear engineering applications. In other fields of applications, the notion of saturation may be preferred, especially when the flow does not involve a gaseous phase (liquid-liquid flows, for instance). Saturation of phase n is defined as the volume fraction of the pore space occupied by phase n. Thus, in gas-liquid flows, the void fraction α is obviously equal to the gas saturation S_g, while the liquid saturation S_l is equal to $1-\alpha$.

Table 1
Generalized Ergun models without interfacial drag.

Model	Lipinski (1981)	Reed (1982)	Hu and Theofanous (1991)
K_g	α^3	α^3	α^3
η_g	α^3	α^5	α^6
K_l	$(1-\alpha)^3$	$(1-\alpha)^3$	$(1-\alpha)^3$
η_l	$(1-\alpha)^3$	$(1-\alpha)^5$	$(1-\alpha)^6$
F_i	0	0	0

of friction between the two liquids. If one drops the quadratic term and the friction term in Eqs. (1) and (2), one recovers the classical generalized Darcy's law used extensively in the case of creeping flow dominated by capillary forces, as proposed heuristically by Muskat (1946). The additional terms try to account for inertia and friction effects. As will be discussed later, they do not entirely translate macroscopically the pore-scale physics as emphasized by upscaling theories.

Several expressions, reported in Tables 1 and 2[2], have been proposed for relative permeabilities, relative passabilities and interfacial friction. Relative permeabilities and passabilities are supposed to depend on the void fraction only. Interfacial friction, if considered by the model, depends on the void fraction, the velocities, and the physical properties of the fluids. Liquid and gas average pressures are linked by an averaged capillary pressure relation, which is generally assumed to be small for such highly permeable media, thus leading to an identity between liquid and gas pressure gradients:

$$\frac{\partial \langle p_l \rangle^l}{\partial z} = \frac{\partial \langle p_g \rangle^g}{\partial z}. \tag{3}$$

Similar approaches have been used in petroleum engineering applications for describing high velocity flows in fractures or near wellbores (Evans and Evans, 1988; Evans et al., 1987; Liu et al., 1995). Some attempt has also been made to adapt the Lockhart–Martinelli approach (Lockhart and Martinelli, 1949) to porous media (Fourar and Lenormand, 2001; Fourar et al., 2001). Nowadays, generalized Darcy–Forchheimer models have become the standard approach for high velocity flows in nuclear safety analysis (Bürger et al., 2006; Kulkarni et al., 2010; Naik and Dhir, 1982; Schmidt, 2007), chemical engineering (Nemec et al., 2001; Saez et al., 1986) and petroleum engineering applications (Fourar and Lenormand, 2000; Jamialahmadi et al., 2005).

However, the cases where these models fail to correctly represent the pressure drop velocity and void fraction velocity relationships are frequent, and particularly for nuclear debris beds, as recently pointed out by Taherzadeh and Saidi (2015) and Chikhi et al. (2016). Two reasons may be given to explain this. The first one is related to the current understanding of the upscaling of multi-phase flows in porous media. Indeed, high velocity single-phase flows have received considerable efforts in theoretical analysis during the last decades (Lasseux et al., 2011; Mei and Auriault, 1991; Quintard and Whitaker, 1994a; 1994b; 1994c; 1994d; 1994e; Whitaker, 1986a; 1996; Wodié and Levy, 1991). Results show the existence of several regimes that cannot be represented exactly by a quadratic Forchheimer extension to Darcy's law: departure from linear Darcy's law involves a weakly inertia regime requiring the introduction of a cubic term, fully developed laminar inertia flows may reach a regime close to the classical quadratic Forchheimer law for sufficiently disordered media, but this is in general only an approximation. Indeed, transition regimes or weak turbulent flows as illustrated in Soulaine and Quintard (2014) in the case of structured packings may require the introduction of irrational expressions. The various regimes may be observed experimentally, even in the context of debris beds, as illustrated in Clavier et al. (2015). However, it was also observed that, providing one accepts an approximation of up to 10%, the results for mm to cm particles of nearly spherical shape can be cast into the classical quadratic Forchheimer law. Similar theoretical and experimental support is still lacking for multi-phase flows. In this context, generalized Forchheimer models, introduced on an empirical basis, have been extensively used for their simplicity and convenience, because their degeneration at vanishing liquid and/or air Reynolds number correctly restores Forchheimer's law, considered as an acceptable model in most cases (see above discussion). It is important however to remember that their mathematical structure did not receive as much theoretical understanding as the case of single-phase flows.

The second reason is associated to the lack of relevant and available experimental data. Indeed, validation of two-phase flow pressure drop models requires on-line measurements of pressure drop, velocities and void fraction in representative conditions. Such measurements are difficult, especially for void fractions. As a consequence, very few data have been reported in the literature for flow in highly permeable media. The only relevant data (for inertial two-phase flows in particle beds) have been proposed by Tutu et al. (1983), and contain measurements of pressure drops, gas velocities and void fraction for zero-liquid rate only. Thus, pressure drop models have been validated either in non-representative conditions, for example from low velocity -viscous regime- experiments through sand as in Lipinski (1984), or indirectly, from dry-out heat flux experiments, as in Hu and Theofanous (1991), by coupling the pressure drop model to heat exchange and mass transfer models.

Recently, a new theoretical model has been proposed for inertial two-phase flows in porous media. By applying the volume averaging method on the two-phase Navier–Stokes boundary value problem, and on the basis of previous works by Whitaker (1986b), Torres (1987), Whitaker (1994) and Lasseux et al. (1996) dedicated to viscous two-phase flows in porous media, Lasseux et al. (2008) derived new macroscopic momentum equations for inertial two-phase flows which are written as

$$\langle \mathbf{v}_l \rangle = -\frac{\mathbf{K}_{ll}}{\mu_l} \cdot \left(\nabla \langle p_l \rangle^l - \rho_l \mathbf{g} \right) - \mathbf{F}_{ll} \cdot \langle \mathbf{v}_l \rangle + \mathbf{K}_{lg} \cdot \langle \mathbf{v}_g \rangle - \mathbf{F}_{lg} \cdot \langle \mathbf{v}_g \rangle \tag{4}$$

$$\langle \mathbf{v}_g \rangle = -\frac{\mathbf{K}_{gg}}{\mu_g} \cdot \left(\nabla \langle p_g \rangle^g - \rho_g \mathbf{g} \right) - \mathbf{F}_{gg} \cdot \langle \mathbf{v}_g \rangle + \mathbf{K}_{gl} \cdot \langle \mathbf{v}_l \rangle - \mathbf{F}_{gl} \cdot \langle \mathbf{v}_l \rangle \tag{5}$$

Several assumptions where adopted to arrive at this result. The most drastic, in view of the application to boiling flows, is the assumption of a quasi-steady state at the closure level, i.e., locally at the pore-scale it is assumed that the pressure and velocity fields are not time-dependent and the interface evolves slowly. Such assumptions are at the core of almost all published two-phase flow models. The fact that these models actually work well, at least to some degree of accuracy, lies on the existence of some ergodicity between space and time, which is partially supported by pore-scale experiments (Sapin et al., 2016) and some macro-scale experiments (Chikhi et al., 2016). Unsteady closure and/or macro-scale equations have been proposed in the literature (Cueto-Felgueroso and Juanes, 2009; Gray and Hassanizadeh, 1991; Hassanizadeh and Gray, 1993; Hilfer, 1998; Kalaydjian, 1987; Panfilov and Panfilova, 2005; Quintard and Whitaker, 1990; Reeves and Celia, 1996). They are still in developments and, in addition, they were not developed

[2] The value of n and the expressions of $A(\alpha)$ and $B(\alpha)$ in the Tung&Dhir model depend on α, defining several flow regimes. See Tung and Dhir (1988) for more details.

Table 2
Generalized Ergun models with interfacial drag.

Model	Schulenberg and Müller (1987)	Tung and Dhir (1988)
K_g	α^3	$\left(\frac{1-\varepsilon}{1-\alpha\varepsilon}\right)^{4/3}\alpha^n$
η_g	$\begin{cases}\text{if } \alpha < 0.3: & \alpha^6\\ \text{if } \alpha > 0.3: & 0.1\alpha^4\end{cases}$	$\left(\frac{1-\varepsilon}{1-\alpha\varepsilon}\right)^{2/3}\alpha^n$
K_l	$(1-\alpha)^3$	$(1-\alpha)^3$
η_l	$(1-\alpha)^5$	$(1-\alpha)^3$
F_i	$350\alpha(1-\alpha)^7(\rho_l-\rho_g)g\varepsilon\frac{\rho_l K}{\sigma_{lg}\eta}\left(\frac{\langle v_g\rangle}{\alpha}-\frac{\langle v_l\rangle}{1-\alpha}\right)^2$	$A(\alpha)\left(\frac{\langle v_g\rangle}{\alpha}-\frac{\langle v_l\rangle}{1-\alpha}\right)+B(\alpha)\left(\frac{\langle v_g\rangle}{\alpha}-\frac{\langle v_l\rangle}{1-\alpha}\right)^2$

for inertia flows. Therefore, the *current* most generalized model for our purposes is the one described by Eqs. (4) and (5).

These equations include 8 unknown tensorial functions. $\mathbf{K}_{ll}$ and $\mathbf{K}_{gg}$ are the *permeability tensors*, and represent the main viscous dissipation due to the creeping flow of each fluid phase, i.e., they are equal to the intrinsic permeability tensor when the saturation of the other phase is zero. $\mathbf{K}_{lg}$ and $\mathbf{K}_{gl}$ are the *viscous coupling tensors*, representing the mapping of the creeping flow viscous drag at the liquid-gas interface over the velocity of the other phase. $\mathbf{F}_{ll}$ and $\mathbf{F}_{gg}$ are the main *inertial correction tensors*, i.e., they revert to the one-phase flow term when the saturation of the other phase is zero. Following the above discussion about Forchheimer's correction, these terms do not necessarily depends linearly on the velocity. Indeed, the theory even tells that they may depend also on both velocities. Finally, $\mathbf{F}_{lg}$ and $\mathbf{F}_{gl}$ are the *inertial coupling correction tensors*, representing the mapping onto the other phase velocity of the additional drag due to inertia. All terms depend on saturation and potentially on the velocities. A theoretical relation between the creeping flow viscous terms has been derived by Lasseux et al. (1996):

$$\mu_g\mathbf{K}_{gl}\cdot\mathbf{K}_{ll}=\mu_l\mathbf{K}_{gg}\cdot\mathbf{K}_{lg}^T \tag{6}$$

It should be noted that the contribution of the additional inertial terms can be assumed to be negligible compared to the creeping flow viscous ones when gas and liquid Reynolds numbers are small: a feature that will play an important role in the identification procedure proposed in this paper. All the terms can be determined by resolving complex boundary value problems, which is a difficult task not undertaken so far for complex porous media.

For 1D flows through homogeneous and isotropic media, tensor terms and vectors become scalars, and partial equivalences can be made between this model and the generalized Darcy-Forchheimer model. If we assume quadratic inertia terms, the viscous and inertial dissipation terms can be related to the relative permeabilities and passabilities as follows

$$K_{ll}=KK_l \tag{7}$$

$$K_{gg}=KK_g \tag{8}$$

$$F_{ll}=\frac{\rho_l}{\mu_l}\frac{K}{\eta}\frac{K_l}{\eta_l}\langle v_l\rangle \tag{9}$$

$$F_{gg}=\frac{\rho_g}{\mu_g}\frac{K}{\eta}\frac{K_g}{\eta_g}\langle v_g\rangle \tag{10}$$

From this point of view, Eqs. (4) and (5) may be considered as more general forms of Darcy-Forchheimer models, for multi-dimensional flows and non isotropic or homogeneous media, based on a more elaborated theoretical justification. However, it should be pointed out that the viscous and inertial coupling tensors cannot be written in a consistent manner in terms of the F_i term in Eqs. (1) and (2). Such an equivalence would indeed require the following condition:

$$\begin{aligned}-(1-\alpha)\left[-\mu_l K_{ll}^{-1}\cdot K_{lg}\cdot\langle v_g\rangle+\mu_l K_{ll}^{-1}\cdot F_{lg}\cdot\langle v_g\rangle\right]\\ =\alpha\left[-\mu_g K_{gg}^{-1}\cdot K_{gl}\cdot\langle v_l\rangle+\mu_g K_{gg}^{-1}\cdot F_{gl}\cdot\langle v_l\rangle\right]=\frac{F_i}{\varepsilon}.\end{aligned} \tag{11}$$

This relation requires, to be verified, $F_i=K_{lg}=F_{lg}=K_{gl}=F_{gl}=0$. The two approaches may therefore be compatible when interfacial drag is zero or negligible, i.e. when it is not necessary to use these terms in the models. It should be noted that this situation may correspond to creeping flows in low permeability media, although this remains controversial (Rose, 2000). However, in the case of high permeability media, such as the debris beds considered in this work, observations (Chikhi et al., 2016; Tutu et al., 1983) have shown that coupling terms have a significant influence, even for the small Reynolds numbers, as recently pointed out by Chikhi et al. (2016). Therefore, the drag term in Eqs. (1) and (2) and the coupling terms in Eqs. (4) and (5) are not zero, and Eq. (11) reveals a contradiction between these two approaches, since it would require F_i to be both positive and negative, at least in the Darcy regime, which is impossible. Hence, Eqs. (4) and (5) constitute an original approach in the treatment of interfacial drag in two-phase flows through porous media.

2.2. Adimensionized equations

The 1D form of Eqs. (4) and (5) may be presented in an adimensionalized form, that may be useful to generalize the results. As suggested by several authors (Dye et al., 2013; Nemec and Levec, 2005), they can be re-written in terms of the Reynolds numbers for the liquid phase and the gas phase:

$$Re_\beta=\frac{\rho_\beta d\langle v_\beta\rangle}{\mu_\beta(1-\varepsilon)},\ \beta=g,l, \tag{12}$$

and the Galilei numbers for the liquid phase and the gas phase:

$$Ga_\beta=\frac{\left(\nabla\ p_\beta{}^\beta+\rho_\beta g\right)\rho_\beta d_{St}^3}{\mu_\beta(1-\varepsilon)^3},\ \beta=g,l. \tag{13}$$

The adimensionalized equations, after calculation, are:

$$Re_l=-K_{ll}^*Ga_l-F_{ll}^*Re_l+K_{lg}^*Re_g-F_{lg}^*Re_g \tag{14}$$

$$Re_g=-K_{gg}^*Ga_g-F_{gg}^*Re_g+K_{gl}^*Re_l-F_{gl}^*Re_l, \tag{15}$$

where $K_{\alpha\beta}^*$ are the adimensionalized unknown functionals given by:

$$K_{ll}^*=\frac{(1-\varepsilon)^2}{d_{St}^2}K_{ll}\qquad K_{gg}^*=\frac{(1-\varepsilon)^2}{d_{St}^2}K_{gg} \tag{16}$$

$$K_{lg}^*=\frac{\rho_l}{\rho_g}\frac{\mu_g}{\mu_l}K_{lg}\qquad K_{gl}^*=\frac{\rho_g}{\rho_l}\frac{\mu_l}{\mu_g}K_{gl} \tag{17}$$

$$F_{ll}^*=F_{ll}\qquad F_{gg}^*=F_{gg} \tag{18}$$

$$F_{lg}^{*} = \frac{\rho_l}{\rho_g}\frac{\mu_g}{\mu_l}F_{lg} \qquad F_{gl}^{*} = \frac{\rho_g}{\rho_l}\frac{\mu_l}{\mu_g}F_{gl} \tag{19}$$

The procedure detailed below can be applied either to these adimensionalized equations or to their original dimensional form. For the on-coming developments, the use of the dimensional form (Eqs. (4) and (5)) allows a more clear and direct visualization of the different effects, in particular those of the particle-size and of flow inertia. Therefore, the procedure will be given in the dimensional form. The final model can be transposed in adimensionalized form by use of Eqs. (16)–(19).

2.3. Main issues in model derivation

The main difficulty to obtain a working model from Eqs. (4) and (5) lies in the identification of the 8 unknown functionals of the void fraction α, the velocities $\langle v_l \rangle$ and $\langle v_g \rangle$, the characteristics of the medium (porosity, permeability) and the physical properties of the fluids (viscosities, densities). There have been attempts to work this inverse problem when inertia is negligible, i.e. $F_{ll} = F_{gg} = F_{gl} = F_{lg} = 0$, by use of mathematical methods (Chardaire-Rivière et al., 1992; Chavent et al., 1980; Ewing et al., 1994; Nordtvedt et al., 1993). All these papers have shown that identifying the functionals was a very challenging task. In this work, the higher number of functionals makes the identification even more complicated. In addition, we know that there are several regimes, with different dependencies upon saturation and velocities. It has been found in the case of single-phase flows that a full inverse method with an objective function involving all the regimes may lead to an incorrect identification of some of the regimes. For instance, the linear regime value may be influenced, contrary to the theory, by points in the inertia regimes. This could be avoided by tweaking the objective function, but it was found that this is less accurate and efficient than a separated determination, since we know that the Darcy regime is *independent* of the inertia terms (Clavier et al., 2016). To avoid these difficulties, a segregated identification procedure is proposed in this work. The methodology will be presented in detail and developed in Section 4.

The identification requires experimental databases including measurements of pressure drops, void fractions and velocities, regardless of the method used. Very few data have been reported in the literature for inertial two-phase flows through porous media. Until very recently, in the context of nuclear safety, the only available data were those proposed by Tutu et al. (1983), which contain measurements for zero-net water velocity only. This database was therefore inadequate to identify all the terms of Eqs. (4) and (5). In order to fill this lack of information, an original database has been proposed by Chikhi et al. (2016) for non-zero water velocities.

3. Experimental data

As already explained, the identification of the model requires experimental databases containing measurements of velocities, pressure drops and void fractions. Such data are very scarce, mostly because of the technological difficulty of the void fraction measurement. The only relevant experimental data for this study are those proposed by Tutu et al. (1983) and Chikhi et al. (2016), which involve steady-state air-water flows through single-sized spherical particle beds. In this section, these data will be briefly presented and commented.

Experiments of Tutu et al. (1983) have been performed in zero-net water velocity conditions. Pressure drops and void fractions have been measured for gas velocities ranging from 0 to 0.5 m/s. Three beds have been studied. The diameters of the particles are 3.18 mm, 6.35 mm and 12.7 mm. In experiments of Chikhi et al. (2016), both zero- and non-zero-net water velocities have been investigated. While the gas velocities range from 0 to 0.5 m/s, the water velocities range from 0 to 32 mm/s. Two beds have been studied, with 4 mm and 8 mm particles.

Considering the investigated range of velocities and particle sizes, the corresponding gas Reynolds number is between 0 and 500, while the liquid Reynolds number is between 0 and 300, the Reynolds number for a β-phase ($\beta = l, g$) being defined as Eq. (12).

Fig. 1a presents the pressure drop measurements of Tutu et al. (1983) and those of Chikhi et al. (2016) for zero-net liquid velocity. Pressure drop is normalized by the liquid hydrostatic pressure gradient $\rho_l g$, so that it is equal to 1 for null gas velocity. Each series corresponds to a different particle size. If this normalized pressure drop is smaller than 1, this means that air creates an upwards friction force on water. For low gas velocities, it decreases with the same slope regardless of the particle diameter. After reaching a minimum value, which depends on the particle diameter, it increases and seems to tend to 1 for very high gas velocities, at least for 3.18 mm and 4 mm particles.

Void fraction measurements for zero-liquid velocity experiments are presented in Fig. 1b. As for pressure drops, each series corresponds to a different particle size. It should be noted that the data reported here correspond to global void fractions, i.e., average values in space and time, in steady-state flows. The measurement uncertainty is of the order of $\pm$ 10% for the data of Chikhi et al. (2016), as reported in their article. However, uncertainties are not provided by Tutu et al. (1983) for their data.

Void fraction increases with gas velocity, and the following dimensional correlation is able to predict all data within 10 %:

$$\alpha = 0.83 \langle v_g \rangle^{1/3} \tag{20}$$

This correlation does not involve a parameter depending upon the particle diameter. Given the void fraction measurement incertitude and accuracy, it is not possible to quantify precisely such a dependence. One should remember, however, that a variation of the void fraction by about 0.10 may lead to significant changes in the non-linear parameters involved in the two-phase flow model. Therefore, further improvements in the experimental and identification procedures would be rather interesting from a fundamental and practical point of view.

Results from non-zero water velocity experiments by Chikhi et al. (2016) are presented in Figs. 1c–f.

Figs. 1c presents the pressure drop measurements for 4 mm particle bed. As in Fig. 1a, pressure drop is normalized by the liquid hydrostatic pressure gradient. Each series corresponds to a constant liquid velocity. For low water velocities - $\langle v_l \rangle < 4$ mm/s, or $Re_l < 29$ - a similar behavior to the zero-net water velocity is observed. The pressure gradient first decreases below the hydrostatic pressure gradient with increasing air flow rate. After reaching a minimum, it increases for higher air flow rate. For higher water velocity, the normalized pressure gradient is always greater than 1 and increases continuously with the air velocity.

Void fraction measurements for 4 mm particles are presented in Fig. 1d. As for pressure drops, each series correspond to a constant water velocity. Within the 10 % incertitude, it appears that water velocity has a weak influence on the void fraction, which mainly depends on the gas velocity. Eq. (20) is still acceptable.

Data concerning 8 mm particles are presented in Fig. 1e - pressure drops - and 1 f - void fraction. Similar behaviors to the case of 4 mm particles are observed, and Eq. (20) remains acceptable.

4. Derivation of a new model

The ability of Eqs. (4) and (5) to reproduce the experimental data presented in the previous section will now be assessed, and correlations for viscous and inertial correction terms will be deter-

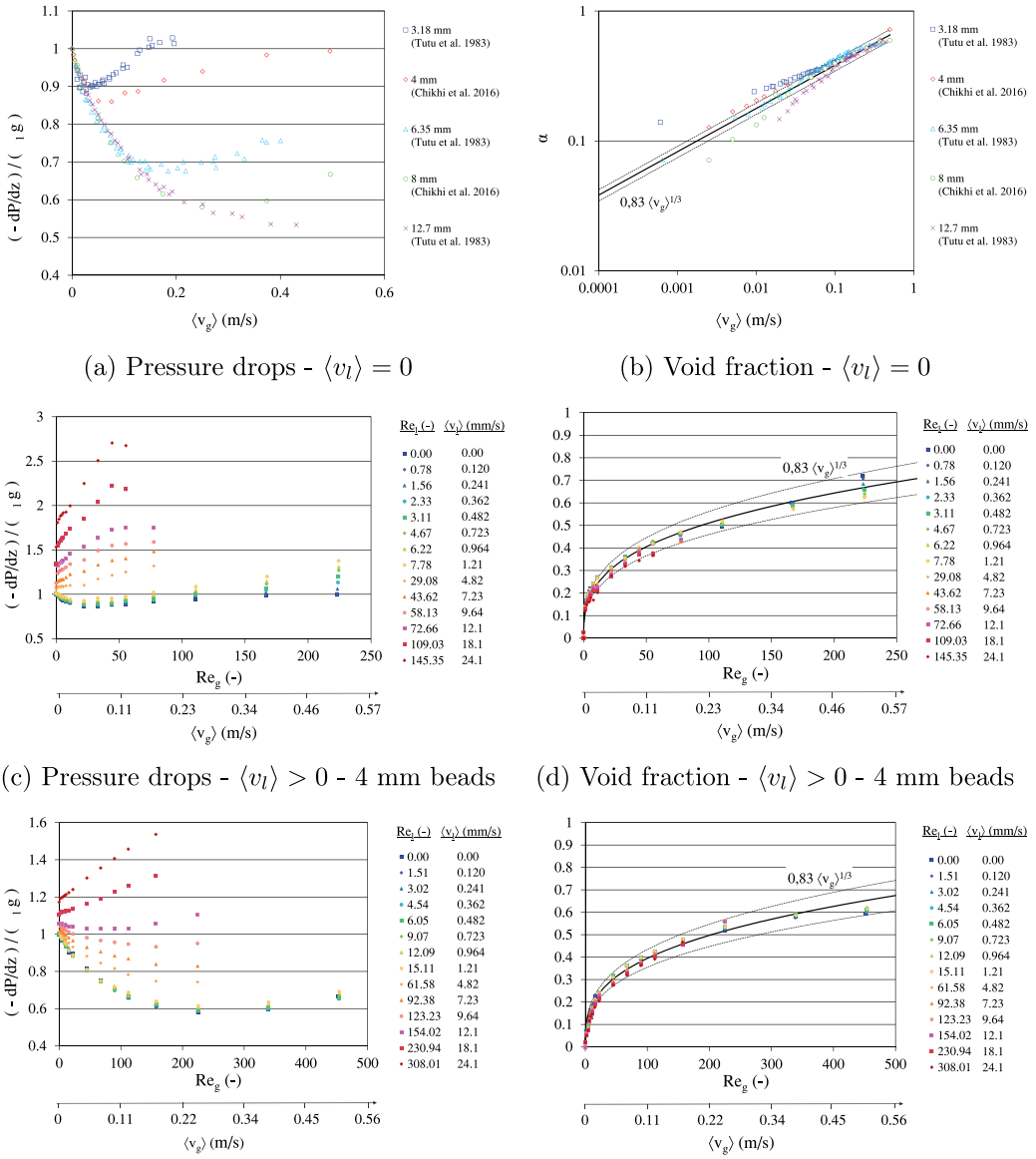

(a) Pressure drops - $\langle v_l \rangle = 0$

(b) Void fraction - $\langle v_l \rangle = 0$

(c) Pressure drops - $\langle v_l \rangle > 0$ - 4 mm beads

(d) Void fraction - $\langle v_l \rangle > 0$ - 4 mm beads

(e) Pressure drops - $\langle v_l \rangle > 0$ - 8 mm beads

(f) Void fraction - $\langle v_l \rangle > 0$ - 8 mm beads

Fig. 1. Experimental data for inertial two-phase flows through spherical particle beds (from Tutu et al. (1983) and Chikhi et al. (2016)).

mined. Eight unknown functionals (Table 3) have to be determined from two equations only.

The method proposed here for their identification is not trivial and is based on strong assumptions that will be detailed in the course of the following developments. The main difficulties are the number of unknown parameters, and the fact that their formal expressions in terms of the flow variables (saturation and velocities) are not *a priori* defined.

Table 3
Unknown terms in Eqs. (4) and (5) to be determined from experiments.

Permeability	Inertial corrections	Viscous coupling	Inertial coupling correction
K_{ll}	F_{ll}	K_{lg}	F_{lg}
K_{gg}	F_{gg}	K_{gl}	F_{gl}

4.1. Initial remarks and assumptions

It is of fundamental importance to make the two following remarks concerning the structure of Eqs. (4) and (5) and the definition of inertial terms.

- Remark 1: In case of zero net water velocity, and since we are interested in 1D flows through isotropic and homogeneous media, these equations simplify into:

$$0 = -\frac{K_{ll}}{\mu_l}\left(\frac{\partial \langle p_l \rangle^l}{\partial z} + \rho_l g \quad + K_{lg}\langle v_g \rangle - F_{lg}\langle v_g \rangle \right) \tag{21}$$

$$\langle v_g \rangle = -\frac{K_{gg}}{\mu_g}\left(\frac{\partial \langle p_g \rangle^g}{\partial z} + \rho_g g\right) - F_{gg}\langle v_g \rangle \tag{22}$$

- Remark 2: Inertia tends to be negligible for sufficiently small Reynolds numbers, or small velocities. Therefore, in that case,

macroscopic equations simplify to:

$$\langle v_l \rangle = -\frac{K_{ll}}{\mu_l}\left(\frac{\partial \langle p_l \rangle^l}{\partial z} + \rho_l g \quad + K_{lg}\langle v_g \rangle \right. \tag{23}$$

$$\langle v_g \rangle = -\frac{K_{gg}}{\mu_g}\left(\frac{\partial \langle p_g \rangle^g}{\partial z} + \rho_g g \quad + K_{gl}\langle v_l \rangle \right. \tag{24}$$

It should be emphasized that, although it is clear that a "small" velocity means that the viscous effects prevail, its precise definition in terms of Reynolds number remains unclear, as the appearance of inertial effects in multi-phase flows through porous media did not undergo enough theoretical and experimental studies. In single-phase flows, it is generally assumed that the viscous regime, or Darcy regime, occurs for Reynolds numbers of the order of 1–10 at maximum (Chauveteau and Thirriot, 1967; Lasseux et al., 2011; Mei and Auriault, 1991), at least for sufficiently disordered media, but there is no proof -experimental or theoretical- that this order of magnitude remains valid for two-phase flows. In the following developments, some values will be proposed for appearance of inertia effects, on the basis of experimental observations, but further theoretical studies should be conducted on these aspects before any definitive conclusion.

The derivation of the model then requires two assumptions for the formal dependence of the unknown terms to velocities and void fraction.

- The form of the permeability and the inertial correction terms is *chosen* so that their behavior correctly restores the Darcy-Forchheimer law in single-phase flows - $\alpha \to 0$ or $\alpha \to 1$, which has been recognized to correctly represent the available data for debris beds with a 10% incertitude Clavier et al. (2016). This implies:

$$K_{ll} = K k_{ll}(\alpha) \qquad \lim_{\alpha \to 0} k_{ll} = 1 \tag{25}$$

$$K_{gg} = K k_{gg}(\alpha) \qquad \lim_{\alpha \to 1} k_{gg} = 1 \tag{26}$$

$$F_{ll} = \frac{\rho_l}{\mu_l}\frac{K}{\eta}\langle v_l \rangle f_{ll}(\alpha) \qquad \lim_{\alpha \to 0} f_{ll} = 1 \tag{27}$$

$$K_{gg} = \frac{\rho_g}{\mu_g}\frac{K}{\eta}\langle v_g \rangle f_{gg}(\alpha) \qquad \lim_{\alpha \to 1} f_{gg} = 1 \tag{28}$$

- To avoid solving an optimization problem in a functional space because of the dependence of the properties on the void fraction (a very difficult or impossible task as discussed above), the forms of viscous terms in the real flow are *supposed* to be similar to their analytical expressions in an annular two-phase viscous flow through a straight vertical capillary tube, derived from the resolution of the Stokes boundary value problem, as represented in Fig. 2:

$$K_{ll} \approx K(1-\alpha)^3 \tag{29}$$

$$K_{lg} \approx \frac{\mu_g}{\mu_l}\frac{(1-\alpha)^2}{\alpha} \tag{30}$$

$$K_{gg} \approx K\alpha^2 \tag{31}$$

$$K_{gl} \approx \frac{\alpha}{1-\alpha} \tag{32}$$

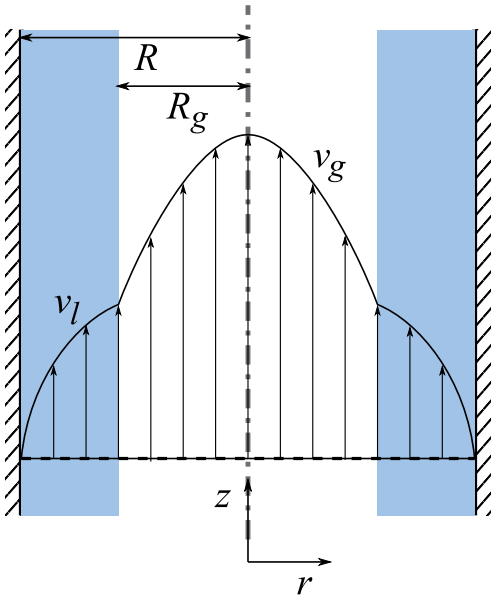

Fig. 2. Annular upwards two-phase viscous flow in a capillary tube.

A theoretical justification of these expressions is provided for instance by Horgue (2012) and Clavier et al. (2015). It should be noted that they verify the theoretical relation between viscous terms (Eq. (6)):

$$\mu_g K_{gl} K_{ll} = \mu_l K_{gg} K_{lg} = K\mu_g \alpha (1-\alpha)^2 \tag{33}$$

4.2. Identification for zero liquid net flow rate

We will first use remark 1 of paragraph 4.1 and consider the simplified macroscopic equations corresponding to $\langle v_l \rangle = 0$. in that case, macroscopic equations can be re-organized as follows:

$$\frac{K_{lg} - F_{lg}}{K_{ll}} = \frac{\frac{\partial \langle p_l \rangle^l}{\partial z} + \rho_l g}{\mu_l \langle v_g \rangle} \tag{34}$$

$$\frac{1 + F_{gg}}{K_{gg}} = -\frac{\frac{\partial \langle p_g \rangle^g}{\partial z} + \rho_g g}{\mu_g \langle v_g \rangle} \tag{35}$$

Several unknown terms still appear in these equations. But for small gas velocities, inertial effects are negligible, which means that F_{lg} and F_{gg} should vanish, and K_{gg} can be identified directly from measurements at zero liquid velocity and small gas velocity. However, an assumption is necessary on either K_{ll} or K_{lg}, since they both are important, even in the viscous regime. In this work, K_{ll} is assumed to be of the form:

$$K_{ll} = K(1-\alpha)^3 \tag{36}$$

This is a strong assumption, but it should be reminded that it corresponds to a relative permeability of a Corey-type equal to $(1-\alpha)^3$, which is used by all the existing models in Tables 1 and 2 and in many other applications (Honarpour et al., 1986). Moreover, this expression is consistent with the limit condition (25) and with the approximated expression (29).

Therefore, the K_{lg} and K_{gg} terms can be identified from experimental data for zero net liquid velocity and small gas velocities. The F_{lg} and F_{gg} terms can be identified afterwards, from zero liquid velocity and high gas velocities experiments.

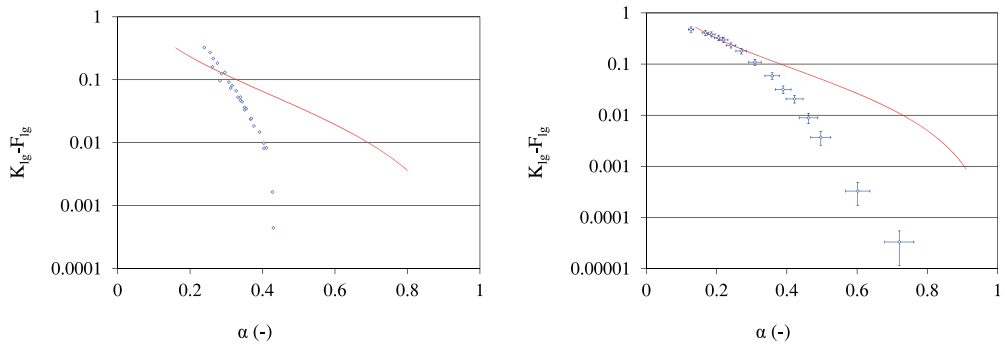

(a) 3.18 mm beads (from Tutu et al. (1983)) (b) 4 mm Beads (from Chikhi et al. (2016))

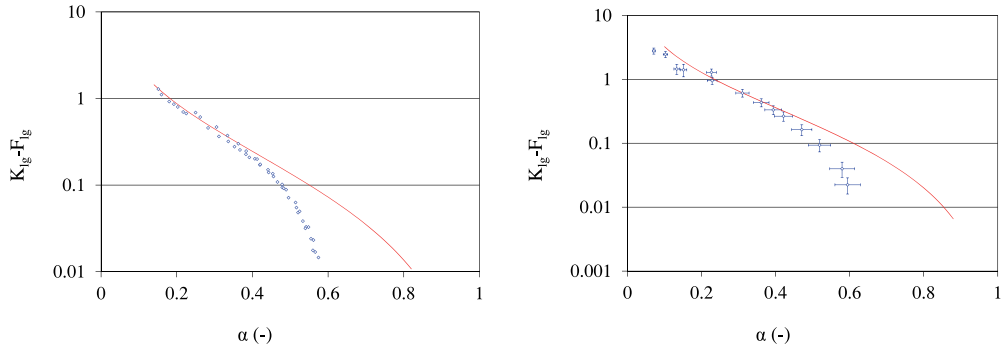

(c) 6.35 mm Beads (from Tutu et al. (1983)) (d) 8 mm Beads (from Chikhi et al. (2016))

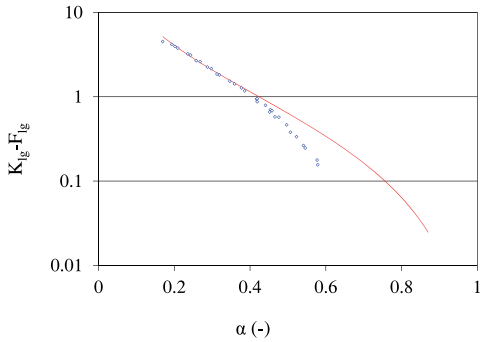

(e) 12.70 mm Beads (from Tutu et al. (1983))

Fig. 3. Identification of cumulated liquid-gas cross terms $K_{lg} - F_{lg}$. Comparison of experimental data (symbols ◇) with Eq. (38) (red curves). The values of the coefficient k_{lg} in Eq. (38) for each bed are reported in Table 4. Note: experimental uncertainties are given for the CALIDE data only (Chikhi et al., 2016), because no informations are provided on that matter in Tutu et al. (1983). (For interpretation of the references to colour in this figure legend, the reader is referred to the web version of this article.)

4.2.1. Identification of K_{lg}

Considering Eqs. (34) and (36), the cumulated influences of K_{lg} and F_{lg} can be directly identified from experiments:

$$K_{lg} - F_{lg} = K(1-\alpha)^3 \frac{\frac{\partial \langle p_l \rangle^l}{\partial z} + \rho_l g}{\mu_l \langle v_g \rangle} \tag{37}$$

Fig. 3 represents the experimental values for $K_{lg} - F_{lg}$ versus the void fraction α. They are obtained from experiments of Tutu et al. (1983) and Chikhi et al. (2016) on single-sized spherical particle beds. Each graph represents data for one size of particle (3.18 mm, 6.35 mm and 12.7 mm for experiments of Tutu et al. (1983) and 4 mm and 8 mm for experiments of Chikhi et al. (2016)). It should be noted that the void fraction is correlated to the gas velocity in these experiments. Thus, small void fractions correspond to small gas velocities, and therefore to weak inertial effects. As explained in the beginning of paragraph 4.2, this means that experimental points for small void fractions, in the graphs of Fig. 3, correspond to K_{lg} only.

Then, once again to avoid optimization over a functional space, an expression close to Eq. (30) is assumed for K_{lg}:

$$K_{lg} = k_{lg} \frac{\mu_g}{\mu_l} \frac{(1-\alpha)^2}{\alpha}. \tag{38}$$

The parameter k_{lg} is determined for each particle size and its values are reported in Table 4. Fig. 3 shows that Eq. (38), represented by red curves, fits very well with experimental data for

Table 4
Best-fitting values of coefficient k_{lg} in Eq. (38).

d (mm)	K (m^2)	k_{lg}	k_{lg}/K
3.18 mm	8.89×10^{-9}	4	4.50×10^{-8}
4 mm	1.21×10^{-8}	5.5	4.56×10^{-8}
6.35 mm	3.18×10^{-8}	15	4.72×10^{-8}
8 mm	5.37×10^{-8}	23	4.28×10^{-8}
12.7 mm	1.96×10^{-7}	70	3.57×10^{-8}

small void fraction, for all particles except the 3.18 mm ones, but overestimates them for higher void fractions. This observation supports the relevance of Eq. (38) to represent K_{lg}, at least for particles larger than 3.18 mm, and suggests that the departure of experimental data from Eq. (38) could be due to inertial effects. Therefore, the F_{lg} term might be identified from the difference between Eq. (38) and experimental data for high void fractions.

The ratio between reported values for k_{lg} and bed permeabilities is almost constant for all particle beds, as shown by the last column of Table 4. This was a predictable result, considering the assumption for K_{ll} and experimental observations (Fig. 1a and b).

4.2.2. Identification of F_{lg}

For high gas velocities and zero water velocity, the pressure drop is calculated by reversing Eq. (21):

$$-\frac{\partial\langle p_l\rangle^l}{\partial z}-\rho_l g=-\frac{\mu_l}{K_{ll}}\left(K_{lg}-F_{lg}\right)\langle v_g\rangle. \tag{39}$$

Experimental data in Fig. 1a, for 3.18 mm and 4 mm particles show that the pressure drop tends towards the liquid hydrostatic pressure gradient $\rho_l g$ for high gas velocities, which means that Eq. (39) tends towards 0. The behavior of pressure drop in 6.35 mm, 8 mm and 12.7 mm particles appears to be similar, although the investigated range of gas velocities is not large enough to confirm this.

Therefore, F_{lg} is determined so that:

$$\lim_{\alpha\to1}-\frac{\mu_l}{K_{ll}}\left(K_{lg}-F_{lg}\right)\langle v_g\rangle=0 \tag{40}$$

Since the limit of K_{ll} is 0 when α approaches 1, a necessary condition - although not sufficient - to verify Eq. (40) is:

$$\lim_{\alpha\to1}K_{lg}-F_{lg}=0. \tag{41}$$

Therefore, we choose to adopt:

$$F_{lg}=K_{lg}f_{lg}, \tag{42}$$

where f_{lg} is an α-dependent function, which verifies:

$$\lim_{\alpha\to0}f_{lg}=0 \qquad \lim_{\alpha\to1}f_{lg}=1.$$

Function f_{lg} is identified for all particle beds in Fig. 4. It appears that the following expression constitutes a good approximation:

$$f_{lg}=\frac{\alpha^3}{\alpha^3+(1-\alpha)^n}, \tag{43}$$

where exponent n depends on the particle size. Its values are summarized in Table 5.

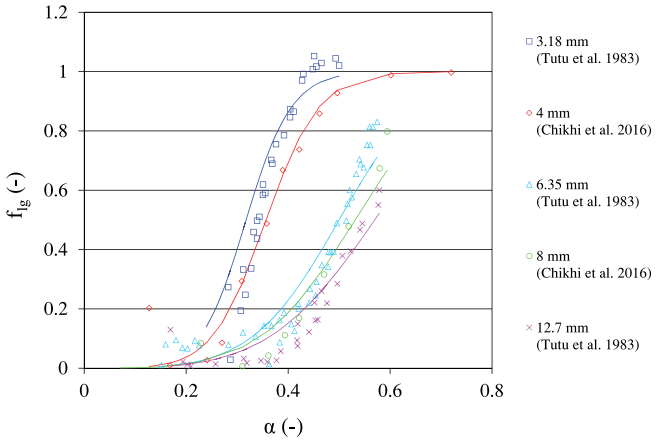

Fig. 4. Identification of the f_{lg} term in Eq. (42) from experimental data.

Table 5
Exponent n in Eq. (43) for all particle beds.

d (mm)	n
3.18	9
4	7
6.35	3.2
8	2.5
12.70	2.2

At this point, it is interesting to point out that since we are dealing here with a term due to inertia effects, there might be an hidden dependence upon the velocity, or velocities, in Eq. (43). Indeed, such a dependence could be recovered by a substitution using Eq. (20). However, there is not enough independent data to validate any expression. This point certainly requires further analysis if additional information can be added.

4.2.3. Identification of K_{gg}

As already explained, K_{gg} is identified from low gas velocity and zero water velocity experiments:

$$-\frac{\frac{\partial\langle p_g\rangle^g}{\partial z}+\rho_g g}{\mu_g\langle v_g\rangle}=\frac{1+F_{gg}}{K_{gg}}\approx\frac{1}{K_{gg}} \qquad (\text{low } \langle v_g\rangle) \tag{44}$$

Fig. 5 summarizes the evolution of Eq. (44) for all particle beds (symbols). Low gas velocity data fit well with the expression $1/K\alpha^4$ (red curves), at least for the smallest particles. This leads to the following Corey formula:

$$K_{gg}=K\alpha^4, \tag{45}$$

For the largest particles, significant differences remain between Eqs. (44) and (45), even for low gas velocities, and Eq. (45) constitutes a limit behavior, when $\langle v_g\rangle$ tends towards 0. But, considering that the Reynolds number increases with the particle size if $\langle v_g\rangle$ is kept constant, inertial effects in the gas phase are likely to be more important for the largest particles, which could explain these differences. Thus, in the same way as for the liquid phase, the difference between experimental data in Fig. 5 and Eq. (45) for high gas velocities is considered as an inertial effect, and is used to identify the F_{gg} term.

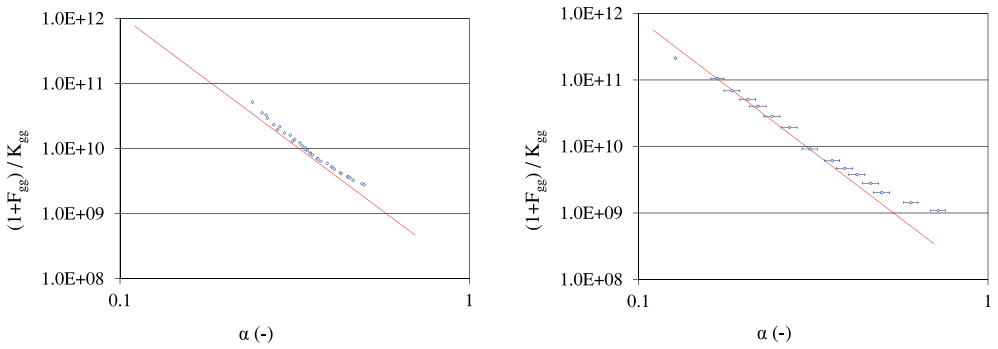

(a) 3.18 mm beads (from Tutu et al. (1983)) (b) 4 mm Beads (from Chikhi et al. (2016))

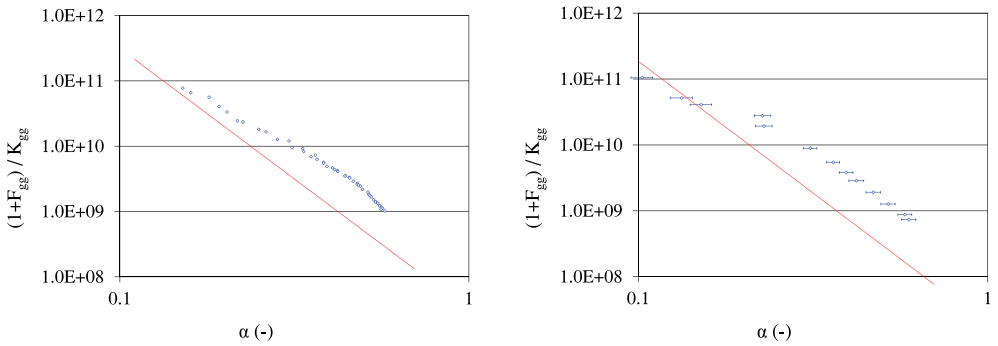

(c) 6.35 mm Beads (from Tutu et al. (1983)) (d) 8 mm Beads (from Chikhi et al. (2016))

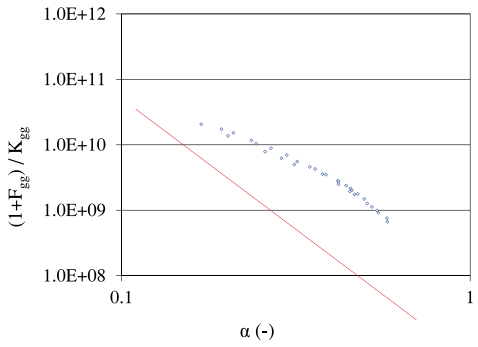

(e) 12.70 mm Beads (from Tutu et al. (1983))

Fig. 5. Experimental identification of expression versus void fraction (symbols ◇) compared to expression for $1/K_{gg}$ (red curves). Note: experimental uncertainties are given for the CALIDE data only, because there are no informations provided on that matter in Tutu et al. (1983). (For interpretation of the references to colour in this figure legend, the reader is referred to the web version of this article.)

4.2.4. Identification of F_{gg}

Given the assumptions made in paragraph 4.1, F_{gg} can be written in the following Forchheimer-like form:

$$F_{gg} = \frac{\rho_g}{\mu_g}\frac{K}{\eta}\langle v_g\rangle \cdot f_{gg}(\alpha), \tag{46}$$

where

$$\lim_{\alpha\to 1} f_{gg}(\alpha) = 1. \tag{47}$$

Function f_{gg} is determined from the difference between Eqs. (44) and (45):

$$F_{gg} = -\frac{\frac{\partial\langle p_g\rangle^g}{\partial z} + \rho_g g}{\mu_g\langle v_g\rangle}K\alpha^4 - 1$$

$$\Rightarrow f_{gg} = \frac{-\frac{\frac{\partial\langle p_g\rangle^g}{\partial z} + \rho_g g}{\mu_g\langle v_g\rangle}K\alpha^4 - 1}{\frac{\rho_g}{\mu_g}\frac{K}{\eta}\langle v_g\rangle}. \tag{48}$$

The evolution of function f_{gg} versus void fraction is presented in Fig. 6, for all particle beds. The limit condition (Eq. (47)) is verified for all particle sizes. This behavior is not a priori guaranteed by Eq. (48), and deserves to be emphasized, since it supports the relevance of the form chosen for F_{gg}, and particularly the factor $\frac{\rho_g}{\mu_g}\frac{K}{\eta}\langle v_g\rangle$ in Eq. (46).

Function f_{gg} depends on void fraction and particle size. However, its behavior can not be reproduced by a simple function of α and d, and only the limit behavior of f_{gg} is implemented in the

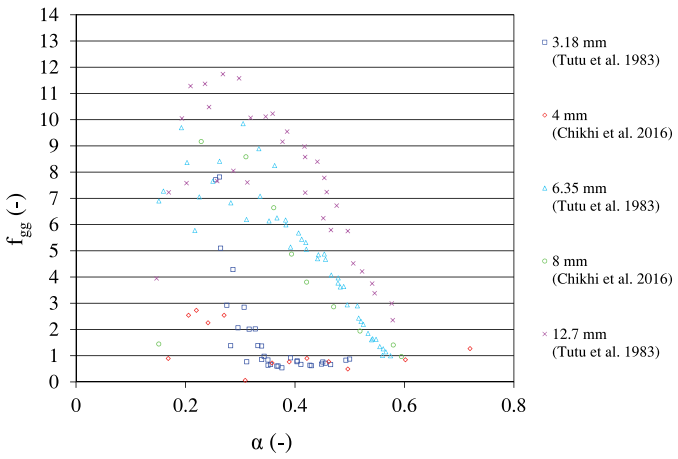

Fig. 6. Identification of the f_{gg} term in equation from experimental data.

final model:

$$f_{gg} = 1. \tag{49}$$

Therefore, the expression for F_{gg} is:

$$F_{gg} = \frac{\rho_g}{\mu_g}\frac{K}{\eta}\langle v_g \rangle \tag{50}$$

This approximation is appropriate for 3.18 mm and 4 mm particles, but the model could be improved for 6.35 mm, 8 mm and 12 mm particle. However, it should be noted that the differences between Eq. (49) and experimental values for f_{gg} could be due to inaccuracies in the modeling of K_{gg}, since the model for K_{gg} also presents significant differences with experimental data for those particles. Furthermore, it is assumed for the identification of f_{gg} that F_{gg} depends linearly on $\langle v_g \rangle$, which could be untrue in certain domains, in the same way that the quadratic dependence of inertial effects to the filtration velocity in single-phase flows is not valid in all flow regimes as discussed before (Clavier, 2015; Firdaouss et al., 1997; Lasseux et al., 2011; Mei and Auriault, 1991; Wodié and Levy, 1991; Yazdchi and Luding, 2012). For these reasons, and in order to prevent the introduction of errors in the model, we recommend anyway the use of Eq. (49), but this point should be further investigated.

In that perspective, a numerical resolution on small representative domains of the pore-scale closure problems given by Lasseux et al. (2008) could help understanding the respective behaviors of K_{gg} and F_{gg}; a detailed analysis which can not be done experimentally. A similar study on single-phase flows has been recently conducted by Lasseux et al. (2011), however, the two-phase flow case is much more challenging.

4.3. Non-zero liquid net flow rate

Assuming that expressions for K_{ll}, K_{lg}, F_{lg}, K_{gg} and F_{gg} established for zero liquid velocity can be applied to non-zero liquid velocities, experimental data for non-zero liquid velocities allow identification of the remaining unknown terms F_{ll}, K_{gl} and F_{gl}. This assumption is verified for viscous terms, which do not depend on velocities, but can be subjected to discussion for inertial terms.

The data used in this paragraph have been obtained by the CALIDE facility (Chikhi et al., 2016). These original data are the only one to propose values for a non-zero liquid net flow-rate.

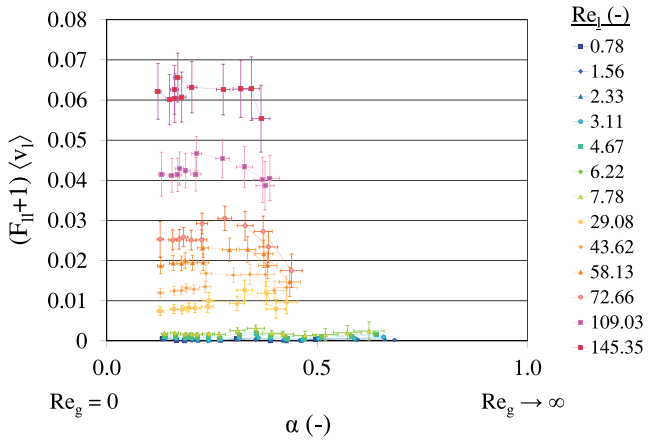

(a) 4 mm beads

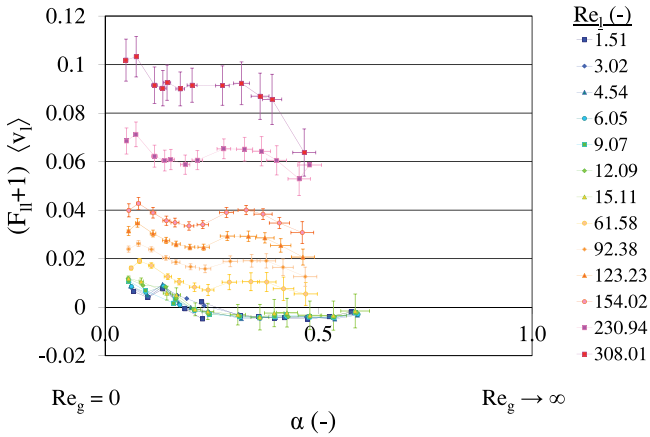

(b) 8 mm beads

Fig. 7. Observation of inertial effects in the liquid phase F_{ll} from pressure drop and void fraction measurements of Chikhi et al. (2016).

4.3.1. Identification of F_{ll}

F_{ll} is the only remaining unknown term in Eq. (4). It can be identified experimentally by:

$$(F_{ll}+1)\langle v_l \rangle = -\frac{K_{ll}}{\mu_l}\left(\frac{\partial P_l}{\partial z} + \rho_l g\right) + \left(K_{lg} - F_{lg}\right)\langle v_g \rangle. \tag{51}$$

This expression is evaluated from experiments and from indentified expressions for K_{ll}, K_{lg} and F_{lg}. The results are presented in Fig. 7a for 4 mm beads and in Fig. 7b for 8 mm beads. In these figures, each series corresponds to the same value for Re_l, while the void fraction, reflecting the influence of Re_g, is reported in the x-axis. The results may be separated in two groups, depending on Re_l.

For $Re_l < 20$, on both Fig. 7a and b, the results are very close to 0. This agrees with theoretical predictions, since inertial effects in the liquid phase should be negligible when Re_l is small. However, this leads to very high relative uncertainties on these results (>100 %), since experimental noise becomes, in proportions, very important. This noise even leads to negative values for expression (51) in Fig. 7b, which is not physical. Hence the data obtained for $Re_l < 20$ should *not* be used to identify F_{ll}, although this term could be non-zero in that domain (inertial effects are known to be potentially significant even for $Re < 20$ in single-phase flows).

For $Re_l > 20$, however, values of expression (51) are higher, which indicates significant inertial effects in the liquid phase. These data are therefore used to identify F_{ll}.

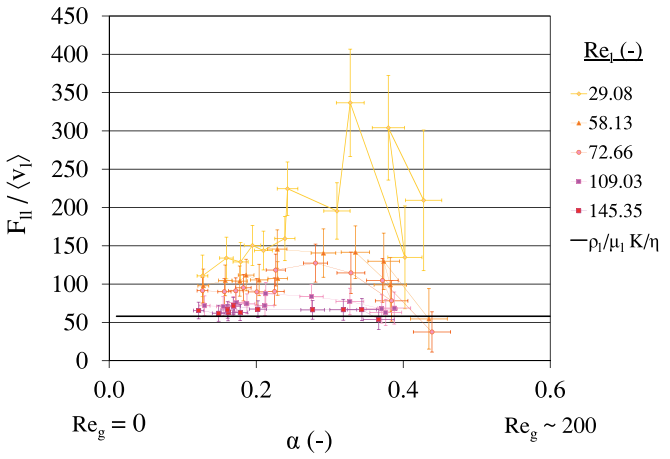

(a) 4 mm beads

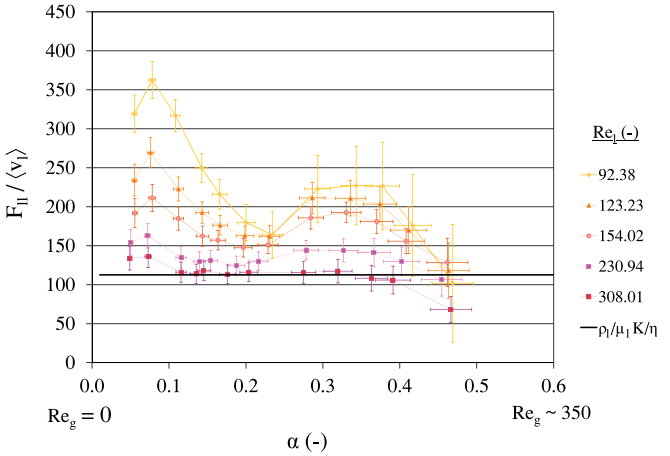

(b) 8 mm beads

Fig. 8. Identification of $F_{ll}/\langle v_l \rangle$.

According to Eq. (27), F_{ll} should be proportional to a function $f_{ll}(\alpha)$, whose limit when α tends to 0 is equal to 1. Fig. 7a and b show that the dependence of F_{ll} on α is weak, at least within the investigated range of void fractions (between 0 and 40 %), which leads us to propose that function f_{ll} should be constant. Then, the constraint on the limit value for f_{ll} when α tends to 0 leads to:

$$f_{ll} = 1. \tag{52}$$

Therefore:

$$F_{ll} = \frac{\rho_l}{\mu_l} \frac{K}{\eta} \langle v_l \rangle, \tag{53}$$

or, equivalently:

$$\frac{F_{ll}}{\langle v_l \rangle} = \frac{\rho_l}{\mu_l} \frac{K}{\eta}. \tag{54}$$

Fig. 8a and b show that this behavior matches the experimental observations for high liquid Reynolds numbers, and for both 4 mm beads and 8 mm beads. Eq. (53) is therefore relevant for high liquid flow-rate, which constitute the general framework of this article, but further studies should be conducted to improve the description of the F_{ll} term for intermediate liquid flows. It is interesting to note here that similar conclusions have been done for inertial effects in the gas phase (F_{gg} term). This shows that the initial assumptions for F_{ll} and F_{gg}, introduced in order to match the behavior of single-phase flows when α tends to 0 or 1, are not entirely verified for all regimes, and that a complete description of pressure drops in two-phase flows requires more complex expressions.

4.3.2. *Identification of* K_{gl}

Since expressions for K_{ll}, K_{gg} and K_{lg} have been obtained, the remaining viscous term K_{gl} can be determined from the theoretical relation of Lasseux et al. (1996) (Eq. (6)):

$$\mu_g K_{gl} K_{ll} = \mu_l K_{gg} K_{lg} \tag{55}$$

$$\Leftrightarrow K_{gl} = \frac{\mu_l}{\mu_g} \frac{K_{gg} K_{lg}}{K_{ll}} = k_{lg} \frac{\alpha^3}{(1-\alpha)}. \tag{56}$$

The validation of this expression requires experimental values for K_{gl}. By reversing Eq. (5), the cumulated influence K_{gl} and F_{gl} is identified:

$$K_{gl} - F_{gl} = \frac{1}{\langle v_l \rangle} \frac{K_{gg}}{\mu_g} \left(\frac{\partial P_g}{\partial z} + \rho_g g \right) + (F_{gg} + 1) \langle v_g \rangle \Big]. \tag{57}$$

Again, inertial effects are assumed to be negligible when velocity is small, i.e. $F_{gl} \ll K_{gl}$ when $\alpha \to 0$. Hence, the experimental values of expression (57) obtained for the small α are attributed to the viscous term K_{gl} only. When α or Re_g increases, on the opposite, inertial effects tend to become dominant. As a consequence, expression (57) should present the following behavior: it should increase from zero when α is very small, then reach a maximum when F_{gl} becomes as large as K_{gl} and finally decrease far below zero as F_{gl} becomes increasingly important.

Fig. 9a and b show the experimental values of expression 57, for 4 mm beads and 8 mm beads. Each series corresponds to the same liquid Reynolds number. For the same reasons as in the determination of F_{ll}, only the data corresponding to $Re_l > 50$ are used. Fig. 10a and b present an enlargement of these figures on the small values of α, where the viscous term K_{gl} should prevail. The observed behavior of expression (57) matches our expectations from previous paragraph, at least for 8 mm particles (Figs. 9b and 10 b). In the case of 4 mm particles (Figs. 9a and 10 a), conclusion is unclear at small α, because experimental uncertainties are very large, but the increase of F_{gl} at high α is very clear.

Comparison between Eq. (56) and experimental values at small α reveals that this correlation fails to predict the results in that domain, at least for 8 *mm* particles (Fig. 10b). In the case of 4 mm particles (Fig. 10a), it might constitute a suitable approximation, but experimental uncertainties prevent any futher conclusion. The reason of this difference could be related to the validity of our hypothesis on inertial effects at small gas Reynolds number: it should be noted that the experimental data used have been acquired at high liquid Reynolds numbers, which could create significant inertial effects even at small gas Reynolds number. An other reason could lie on the postulated expressions for the other viscous terms. This question can not be solved with available data, and clearly appeals for further research. For now, we chose to adopt correlation (56), despite its obvious limitations, for two reasons:

- Since the exact origin of the gap between experiment and Eq. (56), established theoretically, can not be determined, we prefer not to introduce more artificial parameters in the model.

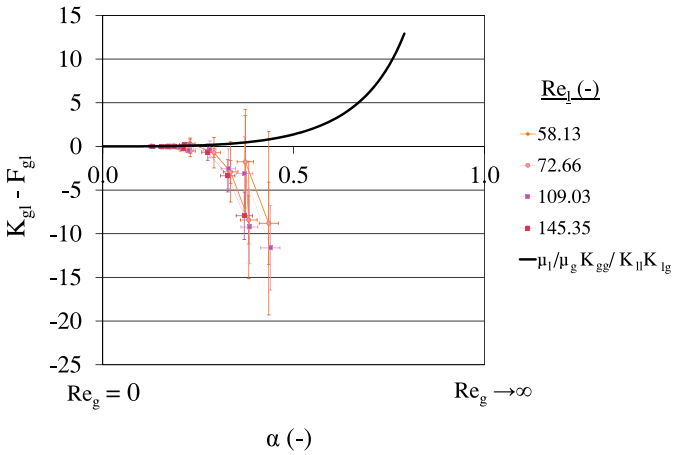

(a) 4 mm beads

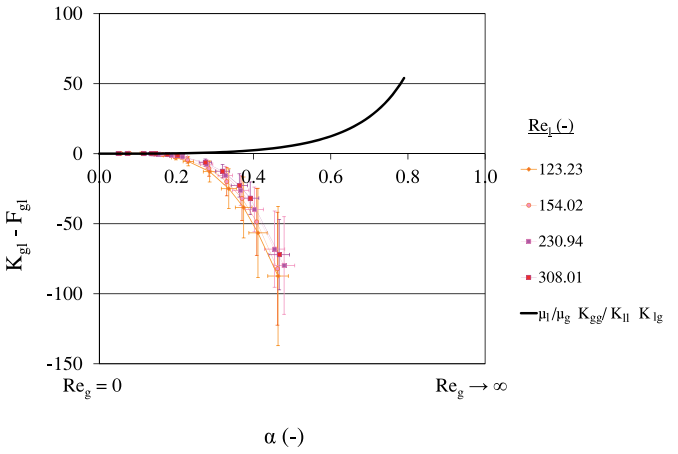

(b) 8 mm beads

Fig. 9. Identification of $K_{gl} - F_{gl}$.

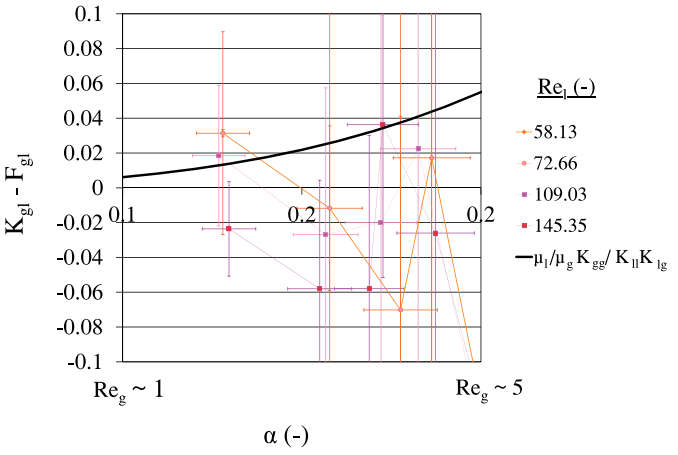

(a) 4 mm beads

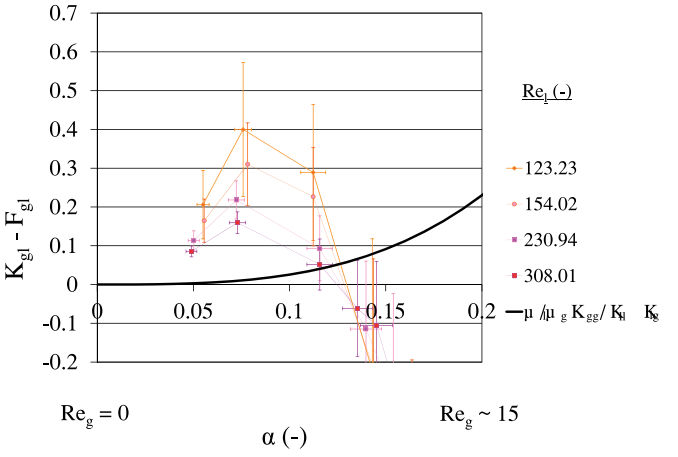

(b) 8 mm beads

Fig. 10. Enlargement of Fig. 9a and b where viscous effects (K_{gl}) are dominant.

- As it will be shown in the next paragraph, the magnitude of F_{gl} at high Re_g is very large compared to the one of K_{gl}. Therefore, the imperfections on the correlation for K_{gl} has a small influence on the determination of F_{gl}.

4.3.3. *Identification of* F_{gl}

The inertial coupling term F_{gl} is identified as the difference between Eqs. (57) and (56) for high gas velocities, which is presented in Fig. 11a and b. Each series corresponds to the same liquid velocity. It is worth noticing that the liquid velocity has very small effects, which supports the relevance of using the expressions for K_{ll}, K_{lg}, F_{lg}, K_{gg} and F_{gg} in non-zero water velocity situations, which is a major assumption made at the beginning of Section 4.3.

Quantitatively, experimental values of F_{gl} present a good agreement with the following correlation:

$$F_{gl} = f_{gl}\alpha^6, \tag{58}$$

where f_{gl} is a constant, which is equal to 3500 for 4 mm beads, and is equal to 7000 for 8 mm beads. This suggests a linear relation between F_{gl} and K/η, but further experimental data, for other particle sizes or shapes are needed in order to comfort this conclusion.

4.4. Synthesis

The method presented in this part, and synthesized in Fig. 12, allowed to identify expressions for unknown terms in averaged momentum equations for inertial two-phase flows through porous media. The model is based on experimental data obtained:

- with beds made of single size spheres (3mm–12mm),
- for liquid Reynolds numbers ranging from 0 to 300,
- for gas Reynolds numbers ranging from 0 to 500.

The resulting model can be summarized as follows:

- Momentum equation for the liquid phase:

$$\langle v_l \rangle = -\frac{K_{ll}}{\mu_l}\left(\frac{\partial \langle p_l \rangle^l}{\partial z} + \rho_l g \quad - F_{ll}\langle v_l \rangle + K_{lg}\langle v_g \rangle - F_{lg}\langle v_g \rangle \right) \tag{59}$$

where:

$$K_{ll} = K(1-\alpha)^3 \qquad K_{lg} = k_{lg}\frac{\mu_g}{\mu_l}\frac{(1-\alpha)^2}{\alpha}$$

$$F_{ll} = \frac{\rho_l}{\mu_l}\frac{K}{\eta}\langle v_l \rangle \qquad F_{lg} = K_{lg}\frac{\alpha^3}{\alpha^3 + (1-\alpha)^n}$$

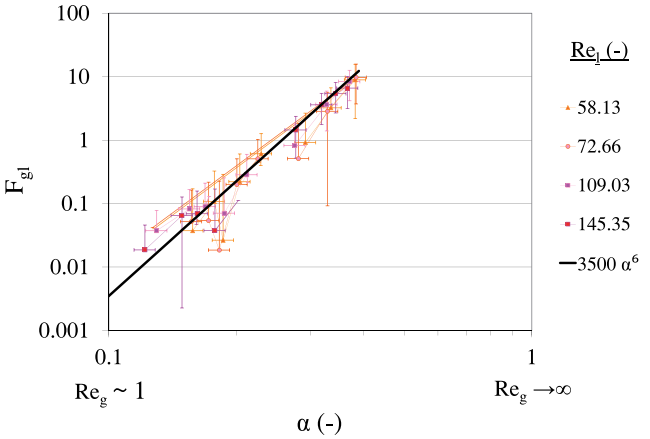

(a) 4 mm beads

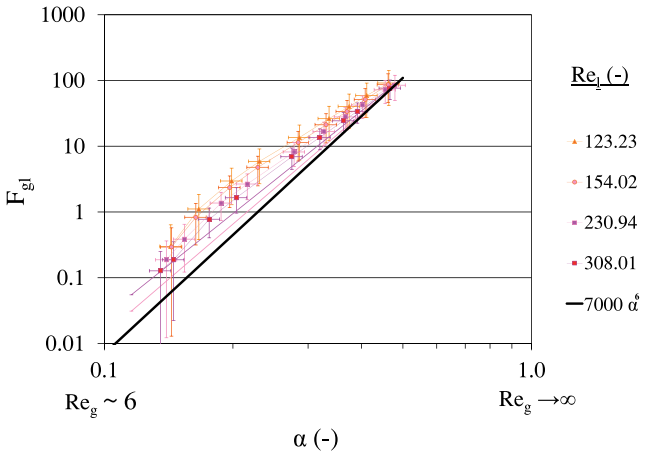

(b) 8 mm beads

Fig. 11. Identification of F_{gl}.

- Momentum equation for the gas phase:

$$\langle v_g \rangle = -\frac{K_{gg}}{\mu_g}\left(\frac{\partial \langle p_g \rangle^g}{\partial z} + \rho_g g \quad - F_{gg}\langle v_g \rangle + K_{gl}\langle v_l \rangle - F_{gl}\langle v_l \rangle \right) \quad (60)$$

where:

$$K_{gg} = K\alpha^4 \qquad K_{gl} = \frac{\mu_l}{\mu_g}\frac{K_{gg}K_{lg}}{K_{ll}}$$

$$F_{gg} = \frac{\rho_g}{\mu_g}\frac{K}{\eta}\langle v_g \rangle \qquad F_{gl} = f_{lg}\alpha^6$$

- Identity between liquid and gas pression gradients (no capillary pressure effect):

$$\frac{\partial \langle p_l \rangle^l}{\partial z} = \frac{\partial \langle p_g \rangle^g}{\partial z} \quad (61)$$

- Permeability and passability (Ergun correlations):

$$K = \frac{d^2\varepsilon^3}{181(1-\varepsilon)^2} \qquad \eta = \frac{d\varepsilon^3}{1.63(1-\varepsilon)}$$

Equivalences can be found between the viscous and inertial dissipation terms and the concepts of relative permeabilities and passabilities of the generalized Ergun models presented in Section 2:

$$K_l = K_{ll}/K = (1-\alpha)^3 \quad (62)$$

$$\eta_l = \frac{\rho_l}{\mu_l}\frac{K_{ll}}{F_{ll}}\frac{\langle v_l \rangle}{\eta} = (1-\alpha)^3 \quad (63)$$

$$K_g = K_{gg}/K = \alpha^4 \quad (64)$$

$$\eta_g = \frac{\rho_g}{\mu_g}\frac{K_{gg}}{F_{gg}}\frac{\langle v_g \rangle}{\eta} = \alpha^4 \quad (65)$$

However, as already pointed out in the introduction, the coupling terms are not consistent with the interfacial friction term proposed in generalized Ergun models, and constitute an original

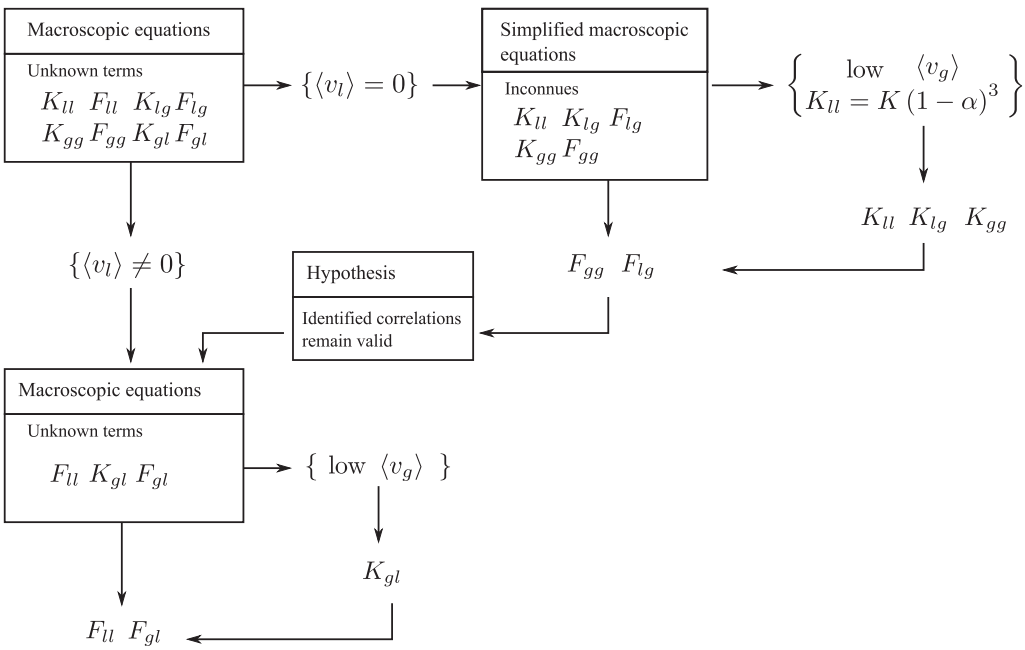

Fig. 12. Schematic representation of the procedure for the identification of the unknown terms in the macroscopic equations.

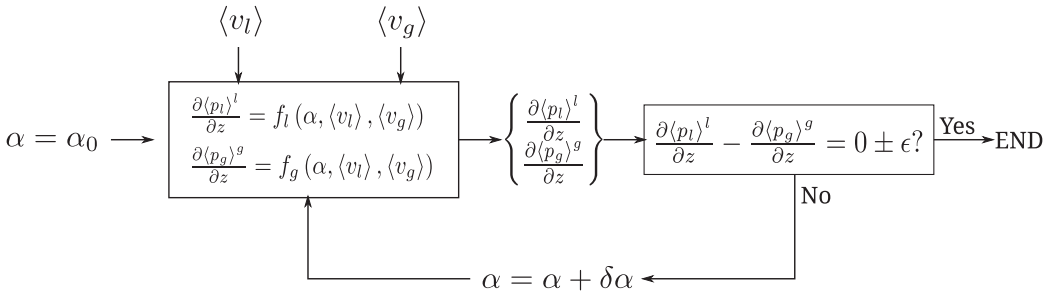

Fig. 13. Schematic representation of the iterative process used to determine the prediction of pressure drop and void fraction by the models.

approach in the modeling of gas-liquid friction in this kind of media. Formal dependences of these terms on the granulometry of the particles are proposed. Thus, the coefficient k_{lg} is proportional to K, as shown in Table 4, and exponent n in expression of F_{lg} also depend on the bed permeability, as shown in Table 5. These recommendations match the observations for 5 sizes of spherical particles, whose diameters range from 3.18 mm to 12.7 mm. The coefficient f_{gl} is proportional to K/η, which match the observations of non-zero net liquid rate flows through 4 mm and 8 mm particle beds. However, more experimental data concerning other sizes or shapes of particles are needed in order to support this recommendation.

5. Validation of the model

In this Section, a two-step validation of the new model is presented. First, the ability of the new model to predict pressure drop and void fraction is assessed, by comparison with experimental data presented in Section 3. Then, the new model is compared to previous models based on a generalization of Ergun law possibly including an explicit term for the interfacial drag.

5.1. Prediction of pressure drop and void fraction

All existing models, including the one proposed in this work, involve two averaged momentum equations, and a capillary-pressure relation. This can be formalized by:

$$\frac{\partial \langle p_l \rangle^l}{\partial z} = f_l(\alpha, Re_l, Re_g) \tag{66}$$

$$\frac{\partial \langle p_g \rangle^g}{\partial z} = f_g(\alpha, Re_l, Re_g) \tag{67}$$

$$\langle p_l \rangle^l - \langle p_g \rangle^g = f_{cap}(\alpha) \Rightarrow \frac{\partial \langle p_l \rangle^l}{\partial z} = \frac{\partial \langle p_g \rangle^g}{\partial z} \tag{68}$$

where f_l and f_g are characteristic functions of the model, and f_{cap} represents the dependence of the capillary pressure on the void fraction.

When liquid and gas Reynolds numbers are imposed, these equations constitute a 3-equations and 3-degrees-of-freedom system (liquid and gas pressure drops and void fraction). By use of an iterative process, it is therefore possible to determine at least one set ($\langle p_l \rangle^l$, $\langle p_g \rangle^g$, α) solution of the system, and verifying the physical condition $0 < \alpha < 1$. The iterative process used in this work (see Fig. 13) is based on the "Goal Seek" function of the MS-Excel® Software. It determines simultaneously, for given liquid and gas Reynolds numbers, the liquid and gas pressure drops and the void fraction so that the capillary pressure relation is verified (identity between liquid and gas pressure drops).

This methodology is the only way to determine the pressure drop and/or the void fraction from the gas and liquid Reynolds numbers only, which are the only input parameters of the model in most applications. The major consequence of this is that predictions of pressure drops and void fractions are linked by the model and have a mutual influence on each other. Hence, the validation of a model requires accurate predictions of both pressure drop and void fraction.

5.2. Comparison between the model predictions and experimental data

By use of the iterative process schematized on Fig. 13, pressure drop and void fraction predicted by the new model are determined, and compared to experimental data in Fig. 14 for 4 mm particles and in Fig. 15 for 8 mm particles.

The prediction by the new model is very accurate in the case of 4 mm particles, as shown by Fig. 14. The dependence of the void fraction to the gas Reynolds number is well reproduced, and its relative independence with the liquid Reynolds number is restored. The behavior of pressure drop is predicted with high precision, for small - or null - as well as for high liquid rate flows.

When both liquid and gas Reynolds numbers are high, pressure drop tends to be slightly overestimated by the model. This is due to a very slight overestimation of the void fraction in this domain. Indeed, Fig. 16 shows that when the measured value of the void fraction is used in the model, instead of the predicted one, the inflexion of the pressure drop for high liquid and gas flow-rates is correctly restored. This is suggesting the following remarks. Firstly, this illustrates the mutual influence of the predictions of pressure drop and void fraction, as discussed in paragraph 5.1. Secondly, this indicates that the sensitivity of the pressure drop to the void fraction is very high: a very slight overestimation of the void fraction led to a significant deviation of the pressure drop from experimental data. A very accurate prediction of the void fraction is therefore required (a remark already introduced before in this paper).

In the case of 8 mm particles, the void fraction is correctly predicted for high flow-rates, but is underestimated for intermediate Reynolds numbers (Fig. 15a). Because of the model sensitivity to this parameter, this leads to significant underestimations of the pressure drop in that domain (Fig. 15a), although the general behavior of pressure drops is well reproduced. These deviations are mainly due to the approximations made in the modelling of the gas phase terms, and in particular to the one for F_{gg} in Section 4.2.4, which is not satisfactory for 8 mm particles. This point should be improved in future works.

5.3. Comparison with existing models

The new model will now be compared to the existing ones, presented in Section 2 and Tables 1 and 2. These models are based on a generalization of Ergun's law, and can be formalized by Eqs. (1) and (2).

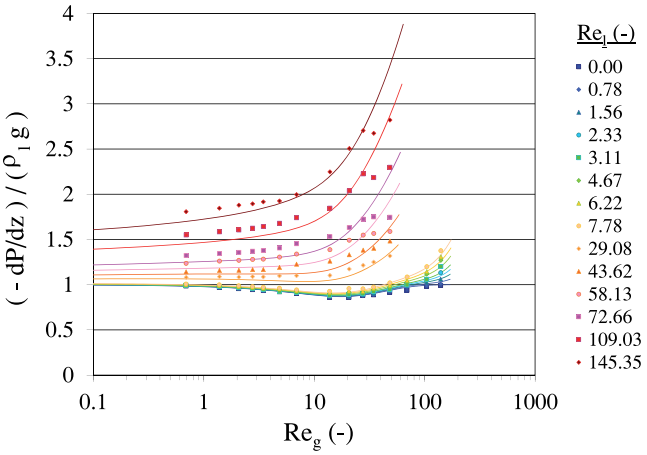

(a) Normalized pressure drop in the liquid phase

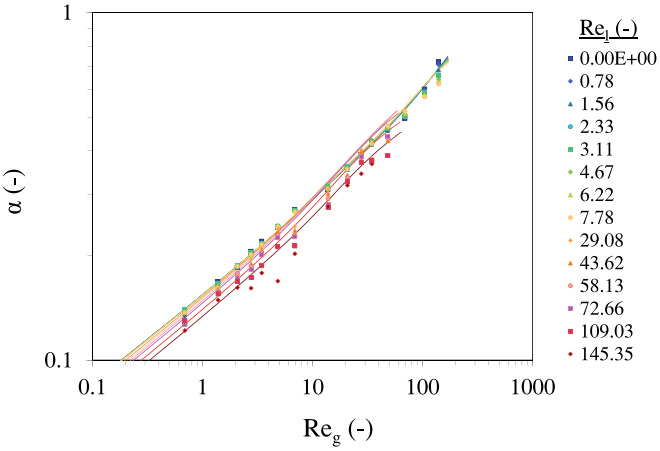

(b) Void fraction

Fig. 14. Direct comparison between predictions of pressure drops and void fraction by the new model and experimental data of Chikhi et al. (2016), for 4 mm beads.

5.3.1. Zero net liquid flowrate

The predictions of normalized liquid pressure drops and void fractions by all generalized Ergun models are compared in Figs. 17a and 17b to those of the new model for zero liquid Reynolds number and 4 mm beads.

The models of Lipinski, Reed and Hu&Theofanous, which do not consider any gas-liquid friction, predict a zero pressure drop and therefore a normalized pressure drop equal to 1, which is inconsistent with the experiments. However, since they involve different expressions for the gas phase relative passabilities, their predictions for the void fraction are not identical, as shown in Fig. 17b: the model of Lipinski underestimates the void fraction, while the model of Reed is accurate for high gas Reynolds numbers only, and the model of Hu&Theofanous underestimates the void fraction for low gas Reynolds numbers and overestimates it for high Re_g.

The model of Schulenberg allows a very accurate prediction of the pressure drop, especially for low gas Reynolds numbers. However, the void fraction is overestimated by this model, which is a problem given the reciprocal influences of these parameters on each other.

The model of Tung&Dhir is able to reproduce quite well the reduction of the pressure drop for low gas Reynolds numbers, but presents very large deviations from experimental data beyond $Re_g \approx 100$. This is due to inacuracies in the modelling of annular flows by Tung and Dhir (1988). Schmidt (2007) attempted to improve the

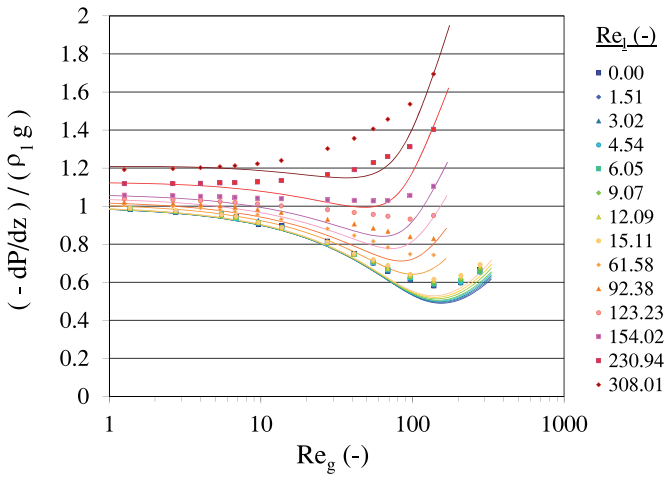

(a) Normalized pressure drop in the liquid phase

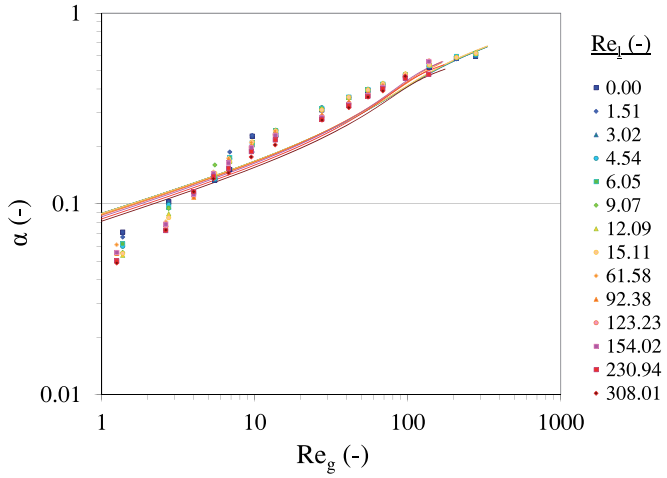

(b) Void fraction

Fig. 15. Direct comparison between predictions of pressure drops and void fraction by the new model and experimental data of Chikhi et al. (2016), for 8 mm beads.

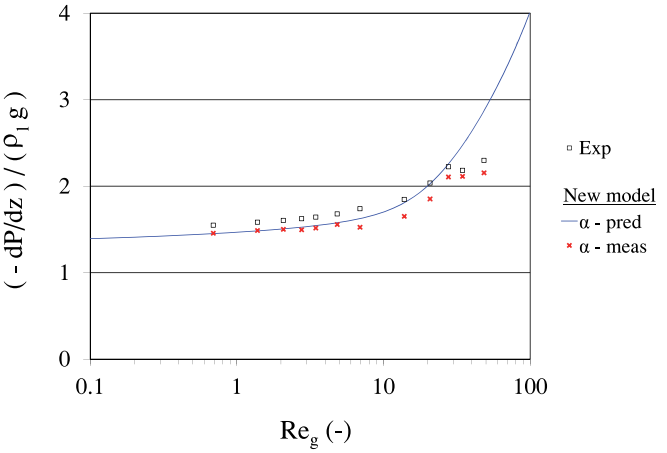

Fig. 16. Influence of void fraction on the prediction of pressure drops, for 4 mm beads.

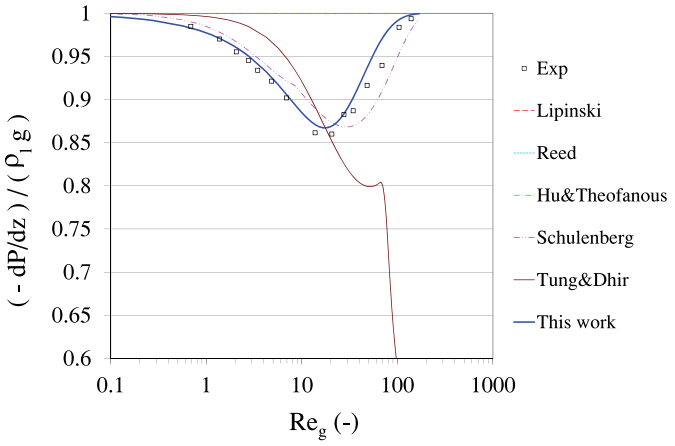

(a) Normalized pressure drop in the liquid phase

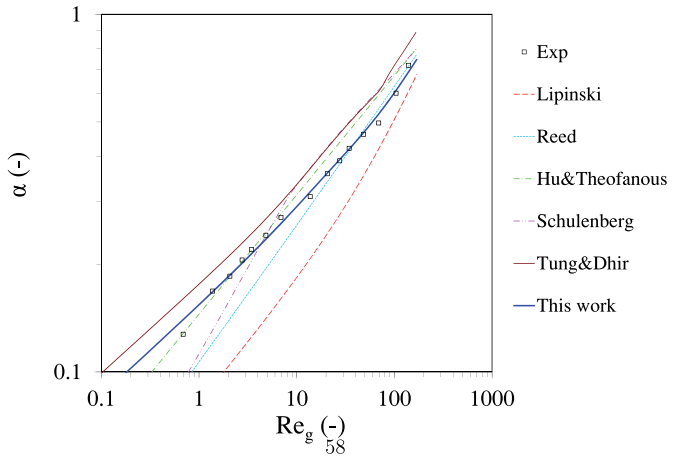

(b) Void fraction

Fig. 17. Comparison of the new model with previously existing ones, for 4 mm beads, $Re_l = 0$.

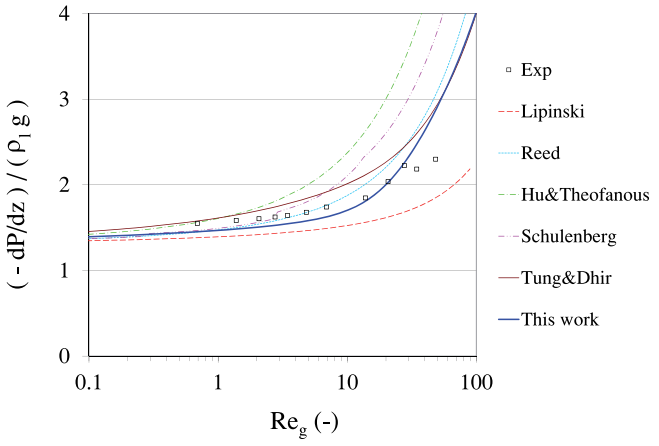

(a) Normalized pressure drop in the liquid phase

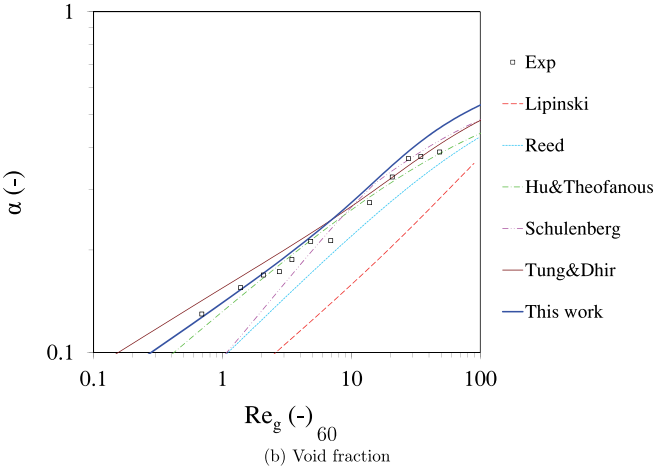

(b) Void fraction

Fig. 18. Comparison of the new model with previously existing ones, for 4 mm beads, $Re_l = 109$.

model by modifying the flow map so that the annular regime is not met. However, the modified model remains less efficient than Schulenberg's in that situation. Furthermore, the void fraction is overestimated.

The new model is the only one to reproduce both pressure drop and void fraction, and within the whole range of gas Reynolds number. It takes advantage of the void fraction measurement in the CALIDE experiment. And, as pointed out above, the pressure drop is very sensitive to the void fraction.

5.3.2. High liquid flow-rate

As an illustration of the performances of the models for high-liquid flow-rates, Fig. 18 compares the models to experimental data for 4 mm beads and $Re_l = 109$.

The model of Lipinski largely underestimates both pressure drop and void fraction. The models of Hu&Theofanous predicts accurately the void fraction, but largely overestimates the pressure drop. The model of Reed allows a better prediction of the pressure drop, at least for moderate gas Reynolds numbers, but underestimates the void fraction.

The model of Schulenberg does not predict well the pressure drop and the void fraction at the same time: only pressure drop is well predicted for low Re_g, while only void fraction is reproduced for high Re_g.

The model of Tung&Dhir very accurately predicts the void fraction, and slightly overestimate the pressure drop. It is the best one among the "generalized Ergun" models under these hydrodynamic conditions.

The new model allows the best prediction of the void fraction for low Re_g, and is very close - although not the best one - for high Re_g. Pressure drop is predicted well, except for the highest Re_g. As already pointed out in paragraph 5.2, the prediction of the pressure drop in that domain could be improved if the void fraction was better reproduced, which could be achieved by a better modelling of inertial effects in the gas phase.

In summary, the new model allows good predictions of pressure drop and void fractions within the whole range of investigated velocities. It represents a significant improvement over the usual generalized Ergun models.

6. Conclusions

Motivated by the reduction of uncertainties in nuclear debris bed coolability assessment, the CALIDE research program has been launched at IRSN (France) in order to better understand, model and predict the pressure drops and the void fractions in inertial two-phase flows in porous media. In the scope of this program, and in order to fill the lack of information in the literature on that subject, an original experimental database containing measurements of pressure drops, average velocities and void fractions has been created. These data have emphasized some lack of predictability of the current models, which are based on a generaliza-

tion of the Darcy–Forchheimer law to multi-phase flows. In this article, the ability of new equations to reproduce these data has been assessed. These equations have been obtained after recent developments in theoretical averaging of two-phase momentum equations in porous media. The model involves eight effective parameters, representing the drag forces due to viscous and inertia effects at the various interfaces. In particular, cross-terms associated to the friction between the phases are shown to play a very important role.

An original method has been proposed to identify analytical expressions for the eight unknown terms in the new averaged equations. This method is not trivial, and strong hypothesis have to be made in order to separate the different physical effects. The consequences of these hypothesis on the physical meaning of the final model have been discussed. As a result, a new analytical model has been proposed to predict the pressure drop and the void fraction in inertial two-phase flows in porous media. The resulting model can be summarized as follows:

- Momentum equation for the liquid phase:

$$\langle v_l \rangle = -\frac{K_{ll}}{\mu_l}\left(\frac{\partial \langle p_l \rangle^l}{\partial z} + \rho_l g \right) - F_{ll}\langle v_l \rangle + K_{lg}\langle v_g \rangle - F_{lg}\langle v_g \rangle \quad (69)$$

where:

$$K_{ll} = K(1-\alpha)^3 \qquad K_{lg} = k_{lg}\frac{\mu_g}{\mu_l}\frac{(1-\alpha)^2}{\alpha}$$

$$F_{ll} = \frac{\rho_l}{\mu_l}\frac{K}{\eta}\langle v_l \rangle \qquad F_{lg} = K_{lg}\frac{\alpha^3}{\alpha^3 + (1-\alpha)^n}$$

- Momentum equation for the gas phase:

$$\langle v_g \rangle = -\frac{K_{gg}}{\mu_g}\left(\frac{\partial \langle p_g \rangle^g}{\partial z} + \rho_g g \right) - F_{gg}\langle v_g \rangle + K_{gl}\langle v_l \rangle - F_{gl}\langle v_l \rangle \quad (70)$$

where:

$$K_{gg} = K\alpha^4 \qquad K_{gl} = \frac{\mu_l}{\mu_g}\frac{K_{gg}K_{lg}}{K_{ll}}$$

$$F_{gg} = \frac{\rho_g}{\mu_g}\frac{K}{\eta}\langle v_g \rangle \qquad F_{gl} = f_{lg}\alpha^6$$

- Identity between liquid and gas pression gradients:

$$\frac{\partial \langle p_l \rangle^l}{\partial z} = \frac{\partial \langle p_g \rangle^g}{\partial z} \quad (71)$$

- Permeability and passability (Ergun correlations):

$$K = \frac{d^2\varepsilon^3}{181(1-\varepsilon)^2} \qquad \eta = \frac{d\varepsilon^3}{1.63(1-\varepsilon)}$$

The comparison of the predictions of this model with experimental data demonstrated its predictability, within the whole investigated range of liquid and gas Reynolds numbers, which covers 0 to 300 for the liquid phase, and 0 to 500 for the gas phase. Although some improvements are still needed, in particular for the modeling of inertia effects in the gas phase, the comparison with existing models showed that the new model represents a significant improvement in the description of high velocity multi-phase flows in particle beds.

Further improvements can be achieved in several directions. First, it must be remembered, as emphasized in the paper, that several assumptions were made in the theoretical development: decoupling between closure problems for momentum and heat transfer, quasi-steady closure problems, to name the most important. Second, the identification of the several *functions* of void fraction and (potentially) velocities was achieved by assuming forms of these functions, thus allowing for an optimization procedure carried on only a few scalar parameters. As a consequence, one may miss some physical correlations, in particular with velocities since the gas velocity is loosely correlated to the void fraction in our experiments. A better identification procedure is a challenging mathematical task that could be improved by:

- a better understanding of the functional dependence of the effective parameters, possibly by numerical solutions of the closure problem over realistic pore structures (a very difficult task!),
- more accurate experimental data, for instance following the transient establishment of the steady-state situation.

Acknowledgment

The authors gratefully acknowledge the anonym reviewers of this article for their time and constructive suggestions, which have allowed significant improvements in this work. IRSN and EDF are gratefully aknowledged for their financial support.

References

Broughton, J., Kuan, P., Petti, D., Tolman, E., 1989. A scenario of the three mile island unit-2 accident. Nucl. Technol. 87, 34–53.

Bürger, M., Buck, M., Schmidt, W., Widmann, W., 2006. Validation and application of the WABE code: investigations of constitutive laws and 2D effects on debris coolability. Nucl. Eng. Des. 236, 2164–2188. doi:10.1016/j.nucengdes.2006.03.058.

Chardaire-Rivière, C., Chavent, G., Jaffre, J., Liu, J., Bourbiaux, B., 1992. Simultaneous estimation of relative permeabilities and capillary pressure. SPE Form. Eval. 7, 283–289. doi:10.2118/19680-PA.

Chauveteau, G., Thirriot, C., 1967. Régimes d'écoulement en milieu poreux et limite à la loi de darcy. La Houille Blanche 2, 141–148.

Chavent, G., Cohen, G., Espy, M., 1980. Determination of relative permeabilities and capillary pressures by an automatic adjustment method. In: SPE Annual Technical Conference and Exhibition, 21–24 September, Dallas doi:10.2118/9237-MS.

Chikhi, N., Clavier, R., Laurent, J.-P., Fichot, F., Quintard, M., 2016. Pressure drop and average void fraction measurements for two-phase flow through highly permeable porous media. Ann. Nucl. Energy 94, 422–432. doi:10.1016/j.anucene.2016.04.007.

Cho, D., Armstrong, D., Chan, S., 1984. On the pattern of water penetration into a hot particle bed. Nucl. Technol. 65, 23–31.

Clavier, R., 2015. Etude expérimentale et modélisation des pertes de pression lors du renoyage d'un lit de débris. Université de Toulouse Ph.D. thesis.

Clavier, R., Chikhi, N., Fichot, F., Quintard, M., 2015. Experimental investigation on single-phase pressure losses in nuclear debris beds: identification of flow regimes and effective diameter. Nucl. Eng. Des. 292, 222–236. doi:10.1016/j.nucengdes.2015.07.003.

Clavier, R., Chikhi, N., Fichot, F., Quintard, M., 2016. Experimental study of single-phase pressure drops in coarse particle beds. Nucl. Eng. Des. doi:10.1016/j.nucengdes.2016.04.032.

Cueto-Felgueroso, L., Juanes, R., 2009. A phase field model of unsaturated flow. Water Resour. Res. 45 (10). doi:10.1029/2009WR007945.

Decossin, E., 1999. Numerical investigations on particulate debris bed coolability: Critical analysis of the silfide experimental project. Ninth International Topical Meeting on Nuclear Reactor Thermal Hydraulics (NURETH-9). San Francisco, California.

Dhir, V., Catton, I., 1977. Study of dryout heatfluxes in beds of inductively heated particles. Technical Report. California University, Los Angeles (USA). Dept. of Chemical, Nuclear, and Thermal Engineering.

Dye, A., McClure, J., Miller, C., Gray, W., 2013. Description of non-darcy flows in porous medium systems. Phys. Rev. E 87. doi:10.1103/PhysRevE.87.033012.

Ergun, S., 1952. Fluid flow through packed columns. Chem. Eng. Prog. 48 (2), 89–94.

Evans, E., Evans, R., 1988. Influence of an immobile or mobile saturation on non-darcy compressible flow of real gases in propped fractures. J. Pet. Technol. 40, 1343–1351. doi:10.2118/15066-PA.

Evans, R., Hudson, C., Greenlee, J., 1987. The effect of an immobile liquid saturation on the non-darcy flow coefficient in poros media. Soc. Pet. Eng. - Prod. Eng. Trans. 283, 331–338. doi:10.2118/14206-PA.

Ewing, R., Pilant, M., Wade, J., Watson, A., 1994. Parameter estimation in petroleum and groundwater modeling. IEEE Computational Science and Engineering 1, 19–31.

Fichot, F., Marchand, O., Drai, P., Chatelard, P., Zabiégo, M., Fleurot, J., 2006. Multi-dimensional approaches in severe accident modelling and analyses. Nucl. Eng. Technol. 38, 733–752.

Firdaouss, M., Guermond, J., Le Quéré, P., 1997. Non linear corrections to Darcy's law at low Reynolds numbers. J. Fluid Mech. 343, 331–350. doi:10.1017/S0022112097005843.

Fourar, M., Lenormand, R., 2000. Inertial effects in two-phase flow through fractures. Oil Gas Sci. Technol. - Rev. IFP 55, 259–268. doi:10.2516/ogst:2000018.

Fourar, M., Lenormand, R., 2001. A new model for two-phase flows at high velocities through porous media and fractures. J. Pet. Sci. Eng. 30, 121–127. doi:10.1016/S0920-4105(01)00109-7.

Fourar, M., Lenormand, R., Larachi, F., 2001. Extending the F-function concept to two-phase flow in trickle beds. Chem. Eng. Sci. 56, 5987–5994. doi:10.1016/S0009-2509(01)00209-3.

Ginsberg, T., Klein, J., Schwarz, E., Klages, J., 1982. Transient core debris bed heat removal experiments and analysis. International Meeting on Thermal Nuclear Reactor Safety. Chicago (USA).

Gray, W.G., Hassanizadeh, S.M., 1991. Unsaturated flow theory including interfacial phenomena. Water Resour. Res. 27 (8), 1855–1863.

Hall, P., Hall, C., 1981. Quenching of a hot particulate bed by bottom flooding: Preliminary results and analysis. European Two-Phase Flow Group Meeting. Holland.

Hardee, H., Nilson, R., 1977. Natural convection in porous media with heat generation. Nucl. Sci. Eng. 63, 119–132.

Hassanizadeh, M., Gray, W.G., 1993. Toward an improved description of the physics of two-phase flow. Adv. Water Resour. 16 (1), 53–67. doi:10.1016/0309-1708(93)90029-F.

Hilfer, R., 1998. Macroscopic equations of motion for two-phase flow in porous media. Phys. Rev. E 58 (2), 2090–2096. doi:10.1103/PhysRevE.58.2090.

Honarpour, M., Koederitz, L., Harvey, A.H., 1986. Relative permeability of petroleum reservoirs. CRC Press, Boca Raton, FL.

Horgue, P., 2012. Modélisation multi-échelles d'un écoulement gaz-liquide dans un lit fixe de particules. Université de Toulouse Ph.D. thesis.

Hu, K., Theofanous, T., 1991. On the measurement and mechanism of dryout in volumetrically heated coarse particle beds. Int. J. Multiphase Flow 17, 519–532. doi:10.1016/0301-9322(91)90047-7.

Jamialahmadi, M., Müller-Steinhagen, H., Izadpanah, M., 2005. Pressure drop, gas hold-up and heat transfer during single and two-phase flow through porous media. Int. J. Heat Fluid Flow 26, 156–172. doi:10.1016/j.ijheatfluidflow.2004.07.004.

Kalaydjian, F., 1987. A macroscopic description of multiphase flow in porous media involving spacetime evolution of fluid/fluid interface. Transp. Porous Media 2 (6), 537–552. doi:10.1007/BF00192154.

Kulkarni, P.-P., Rashid, M., Kulenovic, R., Nayak, A.-K., 2010. Experimental investigation of coolability behaviour of irregularly shaped particulate debris bed. Nucl. Eng. Des. 240, 3067–3077. doi:10.1016/j.nucengdes.2010.05.020.

Lasseux, D., Abbasian, A., Ahmadi, A., 2011. On the stationary macroscopic inertial effects for one-phase flow in ordered and disordered porous media. Phys. Fluids 23. doi:10.1063/1.3615514.

Lasseux, D., Ahmadi, A., Arani, A., 2008. Two-phase inertial flow in homogeneous porous media : a theoretical derivation of a macroscopic model. Transp. Porous Media 75, 371–400. doi:10.1007/s11242-008-9231-y.

Lasseux, D., Quintard, M., Whitaker, S., 1996. Determination of permeability tensors for two-phase flow in homogeneous porous media: theory. Transp. Porous Media 24, 107–137. doi:10.1007/BF00139841.

Lipinski, R., 1981. A one-dimensional particle bed dryout model. Trans. Am. Nucl. Soc. 38, 386–387.

Lipinski, R., 1984. A coolability model for post accident nuclear reactor debris. Nucl. Technol. 65, 53.

Liu, X., Civan, F., Evans, R., 1995. Correlations of the non-darcy flow coefficient. J. Can. Pet. Technol. 34, 50–54. doi:10.2118/95-10-05.

Lockhart, R., Martinelli, R., 1949. Proposed correlation of data for isothermal two-phase, twp-component flow in pipes. Chem. Eng. Prog. 45, 39–48.

Mei, C., Auriault, J., 1991. The effect of weak inertia on flow through a porous medium. J. Fluid Mech. 222, 647–663. doi:10.1017/S0022112091001258.

Muskat, M., 1946. The flow of homogeneous fluids through porous media. J.W. Edwards.

Naik, A., Dhir, V., 1982. Forced flow evaporative cooling of a volumetrically heated porous layer. Int. J. Heat Mass Transf. 25, 541–552. doi:10.1016/0017-9310(82)90057-6.

Nemec, D., Bercic, G., Levec, J., 2001. The hydrodynamics of trickling flow inpacked beds operating at high pressures. the relative permeability concept. Chem. Eng. Sci. 56, 5955–5962. doi:10.1016/S0009-2509(01)00216-0.

Nemec, D., Levec, J., 2005. Flow through packed bed reactors : 2. two-phase concurrent downflow. Chem. Eng. Sci. 60, 6958–6970. doi:10.1016/j.ces.2005.05.069.

Nordtvedt, J., Mejia, G., Yang, P., Watson, A., 1993. Estimation of capillary pressure and relative permeability functions from centrifuge experiments. SPE Reservoir Eng. 8, 292–298. doi:10.2118/20805-PA.

Panfilov, M., Panfilova, I., 2005. Phenomenological meniscus model for two-phase flows in porous media. Transp. Porous Media 58 (1–2), 87–119.

Quintard, M., Whitaker, S., 1990. Two-phase flow in heterogeneous porous media i: the influence of large spatial and temporal gradients. Transp. Porous Media 5, 341–379. doi:10.1007/BF01141991.

Quintard, M., Whitaker, S., 1994. Transport in ordered and disordered porous media 1 : the cellular average and the use of weighting functions. Transp Porous Media 14, 163–177. doi:10.1007/BF00615199.

Quintard, M., Whitaker, S., 1994. Transport in ordered and disordered porous media 2 : generalized volume averaging. Transp. Porous Media 14, 179–206. doi:10.1007/BF00615200.

Quintard, M., Whitaker, S., 1994. Transport in ordered and disordered porous media 3 : closure and comparison between theory and experiment. Transp. Porous Media 15, 31–49. doi:10.1007/BF01046157.

Quintard, M., Whitaker, S., 1994. Transport in ordered and disordered porous media 4 : computer generated porous media. Transp. Porous Media 15, 51–70. doi:10.1007/BF01046158.

Quintard, M., Whitaker, S., 1994. Transport in ordered and disordered porous media 5 : geometrical results for two-dimensional systems. Transp. Porous Media 15, 183–196. doi:10.1007/BF00625516.

Reed, A., 1982. The effect of channeling on the dryout of heated particulate beds immersed in a liquid pool. Massachusetts Institute of Technology Ph.D. thesis.

Reed, A.-W., Bergeron, E.-D., Boldt, K.-R., Schmidt, T.-R., 1986. Coolability of UO_2 debris beds in pressurized water pools : DCC-1 & DCC-2 experiment results. Nucl. Eng. Des. 97, 81–88. doi:10.1016/0029-5493(86)90072-5.

Reeves, P., Celia, M., 1996. A functional relationship between capillary pressure, saturation, and interfacial area as revealed by a pore-scale network model. Water Resour. Res. 32 (8), 2345–2358. doi:10.1029/96WR01105.

Rose, W., 2000. Myths about later-day eextension of darcy's law. J. Pet. Sci. Eng. 26, 187–198. doi:10.1016/S0920-4105(00)00033-4.

Saez, A., Carbonell, R., Levec, J., 1986. The hydrodynamics of trickling flow in packed beds. part i: conduit models. AlChE J. 32 (3). doi:10.1002/aic.690320302.

Sapin, P., Gourbil, A., Duru, P., Fichot, F., Prat, M., Quintard, M., 2016. Reflooding with internal boiling of a heating model porous medium with mm-scale pores. Int. J. Heat Mass Transf. 99, 512–520. doi:10.1016/j.ijheatmasstransfer.2016.04.013.

Schmidt, W., 2007. Interfacial drag of two-phase flow in porous media. Int. J. Multiphase Flow 33, 638–657. doi:10.1016/j.ijmultiphaseflow.2006.09.006.

Schulenberg, T., Müller, U., 1987. An improved model for two-phase flow through beds of coarse particles. Int. J. Multiphase Flow 13, 87–97. doi:10.1016/0301-9322(87)90009-7.

Soulaine, C., Quintard, M., 2014. On the use of Darcy-Forchheimer like model for a macro-scale description of turbulence in porous media and its application to structured packings. Int. J. Heat Mass Transf. 74, 88–100. doi:10.1016/j.ijheatmasstransfer.2014.02.069.

Taherzadeh, M., Saidi, M., 2015. Modeling of two-phase flow in porous media with heat generation. Int. J. Multiphase Flow 69, 115–127. doi:10.1016/j.ijmultiphaseflow.2014.10.013.

Torres, F., 1987. Closure of the governing equations for immiscible, two-phase flows: a research comment. Transp. Porous Media 2, 383–393. doi:10.1007/BF00136443.

Tung, V., Dhir, V., 1986. On fluidization of a particulate bed during quenching by flooding from the bottom. Proc. 6th Inf. Exch. Meeting Debris Bed Coolability. 14-1–14-13

Tung, V., Dhir, V., 1988. A hydrodynamic model for two-phase flow through porous media. Int. J. Multiphase Flow 14, 47–65. doi:10.1016/0301-9322(88)90033-X.

Tutu, N., Ginsberg, T., Chen, J., 1983. Interfacial drag for two-phase flow through high permeability porous beds. Interfacial Transp. Phenom., ASME 37–44.

Tutu, N., Ginsberg, T., Chen, J., 1984. Interfacial drag for two-phase flow through high permeability porous beds. J. Heat Transfer 106, 865–870. doi:10.1115/1.3246765.

Tutu, N., Ginsberg, T., Klein, J., Klages, J., Schwarz, C., 1984. Debris bed quenching under bottom flood conditions (in-vessel degraded core cooling phenomenology) [PWR]. Technical Report. Brookhaven National Lab.

Whitaker, S., 1986. Flow in porous media 1 : a theoretical derivation of Darcy's law. Transp. Porous Media 1, 3–25. doi:10.1007/BF01036523.

Whitaker, S., 1986. Flow in porous media ii: the governing equation for immisible two-phase flow. Transp. Porous Media 1, 105–125. doi:10.1007/BF00714688.

Whitaker, S., 1994. The closure problem for two-phase flow in homogeneous porous media. Chem. Eng. Sci. 49, 765–780. doi:10.1016/0009-2509(94)85021-6.

Whitaker, S., 1996. The Forchheimer equation : a theoretical development. Transp. Porous Media 25, 27–61. doi:10.1007/BF00141261.

Wodié, J., Levy, T., 1991. Correction non linéaire à la loi de Darcy. Compte Rendu de l'Académie des Sciences de Paris t312, série II, 157–161.

Yazdchi, K., Luding, S., 2012. Toward unified drag laws for inertial flows through fibrous media. Chem. Engineering Journal 207, 35–48. doi:10.1016/j.cej.2012.06.140.